RAMSES

RAMSES PROJECT

Grant Agreement n° 308497

WP 4: Climate change scenario for urban agglomerations

D4.3

Urban adaptation effects on urban climate

Reference code: RAMSES – D4.3

This project has received funding from the European Union's Seventh Programme for Research, Technological Development and Demonstration under Grant Agreement No. 308497 (Project RAMSES).

Project Acronym: RAMSES

Project Title: Reconciling Adaptation, Mitigation and Sustainable Development for Cities

Contract Number: 308497

Title of the report: D4.3 Urban adaptation effects on urban climate

Reference code: RAMSES – D4.3

Short description

This report contains the results of the advanced numerical models and on-site measurements on the impacts of adaptation on urban climate through meso and microscale analyses conducted by RAMSES researchers on the case study cities of Antwerp, Paris and Delhi at the mesoscale, and Antwerp and Bilbao at the micro-scale. The outcomes are design and policy guidelines for new and consolidated urban areas.

Authors and co-authors: Gabriele Lobaccaro, Koen De Ridder, Juan Angel Acero, Hans Hooyberghs, Dirk Lauwaet, Wouter Lefebvre, Bino Maiheu, Richa Sharma and Annemie Wyckmans.

Partners owning: NTNU

Contributions: TECNALIA, VITO

Made available to: Public

Versioning

Version	Date	Name, organization
0.1	31.10.2015	NTNU
0.2	12.11.2015	NTNU
0.3	23.11.2015	NTNU
0.4	29.11.2015	NTNU
1.0	16.12.2015	NTNU
1.1	31.12.2015	NTNU
1.2	05.01.2016	NTNU

Quality check

Internal reviewers: Diego, Rybski (PIK); Bin, Zhou (PIK); Alistair, Ford (UNEW) and Guerreiro, Selma (UNEW)

Contents

List of figures

List of tables

List of abbreviations

ACT	Atmospheric Chemical Transport
BEP	Building Effect Parameterization
CFD	Computational fluid dynamics
ECMWF	European Centre for Medium-Range Weather Forecasting
ERSDAC	Earth Remote Sensing Data Analysis Center
EUMETSAT	Europäische Organisation für meteorologische Satelliten
GCM	General Circulation Model
HWDs	Heat Wave Days
Land SAF	Land Surface Analysis Satellite Applications Facility
LST	Land Surface Temperature
LUCY	Large-scale Urban Consumption of energY
MetM	Meso-Meteorological
NDVI	Normalized Difference Vegetation Index
PET	Physiological Equivalent Temperature
PMV	Predicted Mean Vote
SET	Standard Effective Temperature
SUHI	Surface Urban Heat Island
SAF	Satellite Applications Facility
TES	Temperature-Emissivity Separation
UCI	Urban Cold Island
UHI	Urban Heat Island
WBGT	Wet Bulb Globe Temperature
WRFM	Weather Research and Forecasting Model

Executive summary

This report contains the results of advanced numerical modelling and on-site measurements on the impacts of climate change adaptation in urban climate conducted by RAMSES researchers on the case study cities of Antwerp, Paris and Delhi at the mesoscale and Antwerp and Bilbao at the microscale. VITO researchers worked on the cities of Antwerp, Paris and Delhi, while the analyses on the city of Bilbao were conducted by NTNU/TECNALIA. It should be noted that the latter, i.e. the Antwerp/Bilbao microscale case studies, were conducted in close cooperation with the respective municipal administrations.

In the first section, *introduction and scope*, the issues and the challenges of climate change arising from heat waves are described by means of case study cities from the literature review. Based on the challenges that the cities have to face, (i) we defined the scopes of the developed case study cities and (ii) conducted analyses for urban adaptation effects on the urban climate.

The contents are organized by considering two different spatial scales:

- mesoscale, the entire city and its parts;
- microscale, the city quarter, square, urban canopy street, etc.

In the *methodology* section, the most important existing methods and tools for urban climate analysis have been presented. The literature review identified the following elements: (i) the features of the two spatial scales (mesoscale and microscale) and (ii) the tools, methods and approaches used in each spatial scale and in the presented case study cities. At the mesoscale, analyses on the cities of Antwerp, Paris and Delhi were conducted; at the microscale, urban climate simulations were performed on Antwerp and Bilbao.

Regarding the effect of green strategies, the following was completed:

- At the mesoscale, sensitivity simulations and measurements were conducted, based on land-use change scenarios in which urban built-up areas in the model were replaced by green areas. Furthermore, analyses were performed to evaluate the impact of the size of urban park areas with respect to their cooling potential. In addition, a regression-based sensitivity analysis on air temperature versus green areas was conducted in Paris for the summer of 2003.
- At the microscale, simulations and measurements for the urban climate model were conducted in order to calculate the potential adaptation effect of trees in a large square in the centre of Antwerp. A comparative analysis was performed to determine which green strategies can best improve thermal comfort in typical urban canyons in Bilbao.

The *results and discussion* section points out that urban green areas, such as parks and green infrastructure like tree-lined streets, have the potential to reduce the urban heat island (UHI) risk locally and in the nearby areas. At the city scale, the effect of vegetation on thermal comfort appears to be limited, unless the percentage of urban vegetation is radically (and unrealistically) enhanced. Nevertheless, vegetation on the very local scale does have good potential as a cooling measure, especially due to its influence on the radiation fluxes and consequently its effects on thermal comfort.

Based on the conducted measurements and analyses, Deliverable 4.3 proposes a set of general adaptive strategies and design recommendations.

At mesoscale analyses:

- in Antwerp was observed that the presence of large parks in the city centre brings local cooling and their presence is definitely preferable to small parks given that one big park provides a higher cooling effect than many small ones. However, the presence of smaller parks might be important at local scale in order to create cooling spots during heat wave events.
- in Paris was qualitatively and quantitatively confirmed the cooling potential of urban green space. The presence of urban park zone exhibits roughly half the UHI intensity, even if the benefit remains strictly localized in the area of the park and in proximity of built urban areas.
- in the city of Delhi was also confirmed that the presence of larger green areas are preferable in comparison to several distributed green spots, given their higher cooling effect.

At microscale analyses:

- in Antwerp the conducted measurements in summer 2013 during the diurnal cycle confirmed the thermal benefit given by the presence of the Stadspark within the city. It also contributes in reducing consistently the number of UHI events. Furthermore in Groenplaats square in the centre of city showed the importance of planting trees in large urban environments by reducing locally the PMV values due to their shadows.
- in Bilbao was demonstrated that the tree-lined streets provided a cooling effect within the urban canyon in terms of PET reduction and local spatial extent. Furthermore the effect of the green roofs on PET at ground level of the street canyon was also noticeable but it resulted relatively small compared to the presence of grass and trees. Therefore tree-lined streets are preferable to green roofs given their higher cooling effect. Also other urban parameters such as orientation and aspect ratio between height and width of the urban canyons have a considerable influence on thermal comfort at the pedestrian level.

The estimated cooling benefits could not be indifferently extended to all the cities given that they are strictly related to the morphology and the urban density of each specific city, the localization and extension of the green areas, the geometry and the orientations of the urban canyons, the presence of prevalent wind. However, the methodologies used in the case study cities could be replicated in other cities for developing urban green design recommendations to mitigate the urban heat island effect.

1 Introduction and scope

1.1 Issues and challenges of the urban heat island in the urban area

The 21st century can be defined as the first "urban century", with global population projected to reach 8.1 billion in 2025 and 9.6 billion in 2050 [1]. This trend can be expected to continue, and the environmental impact of urban areas is a growing concern [2]. This means that more than half of the world's population will live in cities in the near future. In the global context of climate change, the urbanized areas will be more and more vulnerable to extreme weather conditions [3], which will increase the main climatic risks such as heat waves.

In the last ten years, urban areas have experienced additional heat stress due to the urban heat island (UHI) effect. In a recent study conducted in Berlin, Gabriela and Endlicher [4] found that during heat wave events, mortality rates were higher in the city, especially in the most densely built-up districts. Dousset et al. [5] concluded that for Paris during the summer heat wave of 2003, areas exhibiting the highest remotely sensed night-time infrared surface temperature suffered the highest excess mortality. Again for the 2003 European heat wave, Vandentorren et al. [6] found that heat-related excess mortality was especially high in cities, Paris featuring as the highest with an excess mortality of nearly 140% during the period from 1 to 19 August 2003. Even though this enhanced excess mortality can at least partly be attributed to the vulnerability of the urban population (e.g. larger share of isolated elderly people), increased mortality has also been associated with the urban temperature increment itself [7].

Global climate projections consistently point towards an increase in the number, frequency, and intensity of heat waves [8,9]. Schär et al. [10] have shown that extremely hot summers such as the one in 2003 in Europe are likely to become rather common towards the end of the century.

Heat waves claim more victims than any other weather-related disaster [11]. A striking illustration of this stems from the comparison between the number of victims of Hurricane Katrina in 2005, which amounted to approximately 1,500 deaths [12], and those of the European heat wave of 2003, which was responsible for 70,000 reported heat-related deaths [13]. Often, the health impact of heat waves is minimized by invoking the "harvesting" phenomenon, i.e. the displacement of mortality by days or weeks. However, Saha et al. [14] have shown that, although minor heat wave episodes do induce a fair share of harvesting, this effect decreases as a function of heat wave strength. In particular, for the European heat wave of 2003, Toulemon and Barbieri [15] found that the harvesting effect was modest. They found that of the 15,000 excess deaths in France after the heat wave in the summer of 2003, some 4,000 would have died before the end of 2004 in any event. Statistically, the remaining 11,000 would have lived for another 8 to 11 years. From this data, it was estimated that an equivalent of approximately 100,000 life-years were lost in France alone [7].

Recent studies have demonstrated that the urban temperature increases during the heat waves. Stone [16] investigated the impact of the heat wave that occurred in the second half of July 1999 in the Midwestern USA, with temperatures rising well above 32°C, which resulted in several hundred excess deaths. During this event, the cities of Chicago and St Louis were found to be disproportionally hotter than their rural surroundings, i.e. during the heat wave, the UHI intensity of these cities was higher than average. Li and Bou-Zeid [17] considered a heat wave episode in Baltimore (USA), and likewise found an enhanced difference between urban and rural temperatures, i.e. during the heat wave, the urban–rural temperature contrast itself increased.

Measurements have shown that green areas, such as parks and tree-lined streets, are cooler than other urban locations [18], but this effect is generally local and has little to no impact on temperatures in nearby areas [19]. Fallmann et al. [20] found that the presence of a park in Stuttgart locally cools the air temperature by around 1.5°C. It was also demonstrated that one large park is slightly more efficient than the presence of several small parks with the same equivalent surface area. Schubert et al. [21] reviewed potential greening versus soil sealing in Berlin. They came to the conclusion that 25% extra sealing area induces a temperature increase of 0.82°C, while 15% extra greening corresponds to a temperature decrease of 0.5°C. Therefore, given that the presence of parks and green corridors has become more necessary for cooling the UHI in the built environment, their regulation should be framed in the different urban planning scales [22] [23]. Some studies have demonstrated that, even though the cooling effect of the green parks remains rather circumstantial to the vegetated areas, it can also have benefits for the nearby urban areas around the park [22,24]. Several other studies have also confirmed that both the integration of trees or groups of trees within the urban fabric and the presence of tree-lined streets in the urban canyons have a significant cooling effect in terms of reducing the heat island effect [25,26,27].

Gromke et al. [28] examined the effect on air temperature at ground level provided by the presence of tree-lined streets, green façades and green roofs by using computational fluid dynamics (CFD) simulations. On a typical warm day, the highest impact is made by the presence of tree-lined streets, which cool the temperature by up to 1.5°C. Green façades and green roofs were found to have a benefit of about 0.5°C on local air temperature. The authors noted that the effects were only felt in the direct neighbourhood of the additional green space, so if one wants to achieve a city-wide temperature reduction, a large amount of vegetation is required. Also, vegetation-based measures are only effective when sufficient water is available, which may require irrigation during heat waves.

Vegetation has not only a positive effect on the air temperature, but also on the surface temperature and the heat stress that people experience during the day. In a study on Manchester, Gill et al. [29] found that, on a hot summer day, the surface temperatures in the city centre were 13°C higher than in a nearby forest. A sensitivity analysis showed that an increase of 10% of the amount of green space in the city would decrease the surface temperature by 4°C, while a decrease of 10% would have the reverse effect.

The microclimate also influences decisions on whether to use urban space. Axarli and Chatzidimitriou conducted a study based on bioclimatic criteria for improving pedestrians' thermal comfort using different types of trees, low vegetation, green façades, water elements and different soils [30]. Gehl observed the influence of the microclimate on outdoor activities by counting people sitting on benches in the sun and in the shadow of trees [31]. The study showed a significant impact of local sunny or shady conditions on the desire of people to either stay or leave. Another study conducted in Taiwan investigated people's behaviour in urban outdoor spaces: 93% of people visiting a public square in summer chose to stay in the shade of trees or buildings, indicating the importance of shade in outdoor environments [32].

UHIs also have other impacts on urban residents [32], including modified energy demand (higher in summer, lower in winter), thermal stress especially on pedestrians, increased air pollution formation rates and temperature on the façades, and loss of soil moisture. Some studies underline the benefits of vegetation in American and European cities: the cooling effect created by the shading of the trees during the summer time can create a huge reduction in terms of cooling demands of buildings [33,34], as well as reduce CO_2 emissions and increase thermal comfort. Akbari demonstrated that trees in the urban

environment offer significant benefits in terms of reducing building air-conditioning demand and improving urban air quality by decreasing air pollution [35].

1.2 The role of urban simulation in the urban microclimate analyses

Urban planning strategies are more frequently taking into account the presence of vegetation within the urban environment as a crucial element for improving the quality of urban spaces [36]. In fact, urban processes can create local climate conditions that are divergent from the average and influence directly the population that lives in those areas. Architects, urban planners, landscapers, politicians, developers and engineering firms should be aware that the quality, liveability and vitality of urban spaces and urban climate could be strongly modified in line with their political and design decisions [2,37,38].

All environmental and design aspects significantly influence the relationship between the city and people [39] including their health [40,41]. The recognized added value of making outdoor spaces more attractive for people has become a challenge in urban planning [31,42,43,44]. The variations of sun and shade spaces, and changes in wind speed, air temperature, relative humidity and other characteristics of the urban environment inevitably affect citizens' thermal comfort sensation, given their direct exposure to these factors.

Vegetation plays a significant role in regulating the urban climate, as demonstrated in different studies conducted in the cities affected by UHI [22,45]. Beyond mitigating UHI, the use of vegetation, such as green areas, green roofs and green façades, increases the presence of impervious surfaces, which are able to retain water, thus controlling peak discharge [46,47]. All these strategies have a crucial role in the process of sustainable passive refrigeration in urban planning as well as in increasing the human thermal comfort [25,48,49].

To simulate local conditions, microscale numerical models specifically developed for testing typical artificial urban boundaries are needed. The multitude of different finishing materials and sheltering objects produce a very distinct pattern of different climate conditions, especially within built structures such as street canyons [50]. This happens mostly during the daytime, in which the combination of high temperatures and intense solar radiation create strong problems of heat stress [51]. It is becoming common practice to inform urban planners and decision-makers about the attractiveness and effectiveness of new urban spaces by using modelling and simulation tools. Their use enables the benefits of various design and planning alternatives to be tested, predicted and compared, for example in terms of providing quantitative and qualitative understanding of the relationships between the microclimatic environment, subjective thermal assessment and social behaviour. This process works ideally as support information during the early design phases in order to develop the intervention towards a more sustainable and liveable open space for the public. Environmental modelling tools such as ENVI-met [52], TownScope [53], RayMan [54] and SOLWEIG [55] can help predict climatic conditions. Human physiological modelling tools such as those by Huizenga et al. [56] and Huttner, Bruse et al. [57,58] can also provide assessment of human thermal comfort.

1.3 Aims

This deliverable presents some examples of cooling public spaces and buildings in cities by using green vegetation elements such as parks, green roofs, tree-lined streets and green corridors on different urban scales. The outcomes of experimental campaigns on site were investigated and simulation analyses were conducted to study how the green

infrastructure could affect the local climate in the urban environments of the different analysed cities.

The aims of the deliverable are to:

- identify methods, processes and tools applied in different case study cities to analyse and prevent the risk of the UHI;
- develop design recommendations for mitigating the UHI; and
- explore the feedback between adaptation measures and the urban climate in order to identify potential trade-offs and synergies between different urban planning and design policies.

2 Background of spatial scale modelling and monitoring

In the past decade, various applications, such as simulation analyses and on-site measurements conducted in different climate zones, have produced several research outputs on outdoor thermal comfort in the urban environment. On the one hand, the number of studies focusing on how people's thermal perception influences their behaviour and the use of outdoor spaces has increased [30,31,32,39,40,41,42,43,44], while on the other hand, the interest in proposing sustainable strategies has acquired more dedication from researchers and planning practitioners [22,24,25,26,27,35,45,46,47,48,49,50].

The data provided by on-site measurements, numerical modelling, simulations and other methods of urban climate analysis give significant information that could influence the morphology and the configuration of the urban environment, such as the choice of the finishing material of façades, roofs and paving, and type of urban vegetation and urban fabric [59]. The quantitative information resulting from these methods will support city planners and administrations in developing effective urban climate adaptation policies and strategies.

2.1 Spatial scale of the analyses

The complexity of the calculation of the urban climate parameters requires different numerical models due to the different spatial and temporal scales involved. For example, the spatial scale can vary from a few metres (buildings) to a few kilometres, which requires different models and tools for analysing diverse scales [60].

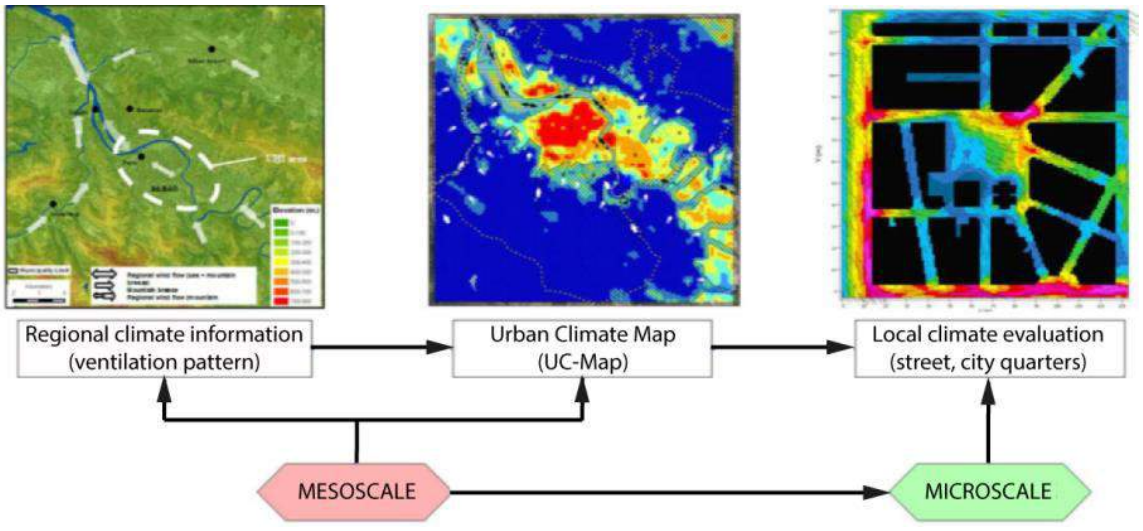

Figure 1 – Multi-scale approach of the urban climate. Steps to evaluate climate in an urban planning context [61].

The use of different spatial scales is extremely important for scale-dependent simplifications. In fact, each model has a specific resolution and grid size in order to solve only a certain level of detail of analysis.

As shown in Figure 1, the spatial scale and the model can vary from (i) a global numerical model with a resolution of a few hundred kilometres (regional and city scale), (ii) to a mesoscale model with a resolution of a few hundred metres (neighbourhood scale), and (iii) to a microscale model with a resolution of a few metres on both the building and urban scale (urban canyon, building scale) [60,61].

2.2 Tools, methods and approaches

The models presented in this section were used for the urban climate analyses and multi-scale studies of the UHI in selected RAMSES cities combining global climate, mesoscale, and microscale models.

Selected tools, methods and approaches for climate analyses at the mesoscale and microscale are described in the following sub-sections. Most of them were used for the microclimate analyses of the case study cities presented in this deliverable.

2.2.1 Mesoscale models and tools

In mesoscale analysis, the city is treated as a whole system interacting with its surroundings, rather than looking at the street-scale level. Mesoscale modelling covers a domain size of typically a few tens of kilometres. The typical grid size varies from regional (up to 100 km or 200 km) to city scale (up to 10 km or 20 km) with a moderate spatial resolution (in the order of 100 m).

2.2.1.1 Satellite thermal image

A *satellite thermal image* maps the UHI by means of thermal infrared satellite imagery that allows the effect of urban climate through land surface temperature (LST) to be analysed.

An example of this technology is the Advanced Spaceborne Thermal Emission and Reflection Radiometer (ASTER). ASTER data is used to create detailed maps of LST, reflectance and elevation. The maps can help to better predict variability and trends in climate, weather and natural hazards [62].

Another example is the use of MODIS Layer Information Moderate Resolution Imaging Spectroradiometer thermal satellite. It displays information on hotspot locations using thermal images collected by the MODIS. The MODIS instrument creates images of the entire surface of the Earth every two days (daily in northern latitudes), making observations in 36 co-registered spectral bands at moderate spatial resolutions (250, 500 and 1,000 metres). Thermal information is collected at 1,000-metres spatial resolution [63].

2.2.1.2 The Weather Research and Forecasting Model

The Weather Research and Forecasting Model (WRFM) is a next-generation mesoscale numerical weather prediction system designed for both atmospheric research and operational forecasting needs. It features two dynamic cores, a data assimilation system and software architecture that facilitates parallel computation and system extensibility. The model serves a wide range of meteorological applications across scales from tens of metres to thousands of kilometres. WRFM can generate atmospheric simulations using real data (observations, analyses) or idealized conditions. WRFM offers operational forecasting a flexible and computationally efficient platform while providing recent advances in physics, and numeric and data assimilation contributed by developers

across the very broad research community. The WRFM model is also used for studying city-scale impacts of UHI in future scenarios [64].

2.2.1.3 UC-Map

The urban climate map, UC-Map, is an important information and evaluation tool for integrating urban climate factors into the urban development strategies. It provides information on climate phenomena and problems in two-dimensional spatial maps [65,66,67,68,69]. The UC-Map has two major components [70]: the Urban Climate Analysis Map (UC-AnMap), which includes climate information describing UHI effects and ventilation patterns, and the Urban Climate Recommendation Map (UC-ReMap), which identifies sensitive climate areas that need specific attention and includes planning advice for mitigating negative climate impacts and strengthening positive ones. One of the most relevant aspects of the UC-Map is that it is based on *Geographic Information Systems* (GIS), enabling integration of climate knowledge into urban planning. The maps have a typical resolution of 100 m [70,71], do not represent a certain climatic condition in a specific period of time, and hence are not fit for studying the local climate phenomena at the microscale. For analyses at the microscale it is necessary to use computational models, such as the *ENVI-met* model [52], which takes into account the interactions between atmosphere, earth surface and all the urban elements.

2.2.1.4 Enviro-HIRLAM

The Enviro-HIRLAM model (Environment-High-Resolution Limited Area Model) is developing an online integrated Meso-Meteorological (MetM) system. By using coupled modelling applications based on numerical weather predictions and an Atmospheric Chemical Transport Model (ACTM), the Enviro-HIRLAM model enables the prediction of atmospheric composition, meteorology and climate change [72,73]. Implementation of ACTM in Enviro-HIRLAM enables inclusion of feedback (regional to urban scale) between the ACTM and numerical weather prediction models [74,75]. The governing equations describing the main processes, such as emissions, advection, horizontal and vertical diffusion, wet and dry deposition, convection and chemistry and aerosol feedback, are solved by the meteorological and chemistry models. The system includes the nesting of domains for higher resolutions, different types of urbanization, and implementation of chemical mechanisms and aerosol dynamics. Enviro-HIRLAM is also coupled with the Building Effect Parameterization module (BEP) [76] and a parameterization of the anthropogenic heat fluxes extracted from the Large-scale Urban Consumption of energY (LUCY) model [77].

A combination of several urban districts that constitutes the city has been represented using BEP. The composition of each district is characterized by a combination of multiple streets and buildings which make up street urban canyons with constant widths but different heights and similar thermo-dynamic characteristics. The contribution of every facet of the urban substrate (street canyon floor, roofs and walls of buildings) is included in the parameterization: heat and turbulent kinetic energy equations are calculated separately as contributions of the vertical surfaces (building walls) as well as horizontal surfaces (floors and roofs).

The anthropogenic heat flux from the global down to the individual city scale at 0.25 arc-minute resolution [77] is simulated by the LUCY model. Information regarding different working patterns, public holidays, vehicle use and energy consumption can be included in the model.

2.2.1.5 UrbClim

UrbClim is a new urban climate model designed to cover mesoscale domains at a spatial resolution of a few hundred metres. This model is a land surface scheme in which the

urban terrain is represented as an impervious slab based on the climate parameters such as albedo, emissivity and aerodynamic and thermal roughness length, and accounting for anthropogenic heat fluxes. UrbClim is coupled to a 3D atmospheric boundary layer module and it is based on simple urban physics. Several validation exercises were conducted for the UrbClim model: Toulouse (France), Ghent and Antwerp (Belgium), Barcelona and Bilbao (Spain), London (UK), Almada (Portugal) and Berlin (Germany). In the analyses, turbulent energy fluxes, wind speed and urban–rural temperature differences were considered. The conducted analyses demonstrated that despite its simplicity, UrbClim has the same level of accuracy than more advanced models [78]. The added value of UrbClim is its computational time that resulted in faster rather than high-resolution mesoscale climate models by about at least two orders of magnitude. This characteristic of the model makes it suitable for long-time integrations in urban climate projections [78].

2.2.2 Microscale models and tools

Microscale simulations consider much smaller domains (a few hundred metres) but employ a much finer spatial resolution (a few metres). Consequently, measurements that aim to cover these variations must be properly and carefully evaluated. In order to estimate effects like pedestrian thermal comfort, the microscale is usually the most relevant scale. However, the main aim of microclimate modelling is to make use of the new ability to observe and analyse consequences of different planning scenarios, as well as to study the impact of the probable increase or decrease in buildings or vegetation due to urban planning.

The typical grid scales in the microscale are neighbourhood scale (up to 1 km or 2 km), and street canyon scale (less than 100 m).

2.2.2.1 Mobile measurements

For local climatological studies, it is common to use either a stationary network of field stations or vehicles equipped with temperature sensors such as mobile measurements.

These measurements have a long tradition: already a century ago, studies used mobile platforms to describe climate variations as well as to study topo-climatology and urban climatology [79]. Mobile measurements have also been used to describe spatial variations in temperature in areas close to roads [80,81].

The advantage of using a mobile platform is that a large area can be covered in a relatively short period and that the same instruments are used. Temperature patterns in relation to topographical factors can be analysed whilst avoiding instrumental errors and calibration.

An important step in the development of the traditional mobile measurements was the inclusion of surface temperature sensors for road climatological studies [82].

2.2.2.2 Observations: in-situ measurements and remote sensing

In-situ-measurements, also identified as in-situ sensing, can be defined as a technology used to acquire information about an object when the distance between the object and the sensor is comparable to or smaller than any linear dimension of the sensor. Networks of *in-situ sensors* have been used for decades in numerous contexts; one of the most prevalent is meteorological stations for collecting climate data.

During the last few years, new monitoring systems (remote sensing) together with wireless telecommunication technologies have advanced at a rapid pace and found new applications. It is becoming increasingly feasible to provide quality-controlled network-

wide data to users via the internet in near real time and this can be assimilated into models within hours with these new technologies [83].

2.2.2.3 ENVI-met

ENVI-met is an example of a widely used urban climate simulation program, specifically developed to study the urban microclimate. This 3D microclimate modelling software, made available free of charge, is used to calculate numerous the meteorological factors as well as comfort quality within an urban area [50,52]. ENVI-met is one of the first models to reproduce the major processes in the atmosphere – including air flow, turbulence, radiation fluxes, air temperature and humidity – on a well-founded physical basis. In ENVI-met, buildings are represented explicitly as obstacles: this feature is completely different to the approach followed in UrbClim, in which the urban substrate is represented as a rough slab.

ENVI-met simulates microclimatic dynamics within a daily cycle in complex urban structures (i.e. buildings of various shapes and heights) as well as vegetation. Its high spatial and temporal resolution enables a fine understanding of the microclimate at street level. This makes ENVI-met a powerful decision support system for urban master planning that takes into account contemporary demands of climate adaptation and mitigation aspects. It is designed for the microscale with a typical horizontal resolution from 0.5 to 10 m. This resolution allows analysis of small-scale interactions between individual buildings, surfaces and plants.

2.2.2.4 TOWNSCOPE

TOWNSCOPE [53] is a digital system developed for conducting solar access analysis in order to support decision-making from a sustainable urban design perspective. The tool, coupled with solar evaluation algorithms, is a three-dimensional urban information system. The 3D models generated by TOWNSCOPE allow the computing of direct, diffuse and reflected radiation in each point. With this data, Fanger's thermal comfort equations [84] can be solved to provide air temperature, relative humidity, ventilation rates and wind speed for any point.

TOWNSCOPE has been coupled with a thermal comfort algorithm, developed by the University of Seville [85] in order to provide urban climate information as described above.

2.2.2.5 RayMan

The RayMan model is used for calculating short- and long-wave radiation fluxes on the human body [86]. Suitable for several applications in urban areas such as urban planning and street design, RayMan enables researchers to work on complex urban structures. The value of mean radiant temperature (T_{mrt}) is the output of the model. This climate parameter is required for the human energy balance model, assessment of the urban bioclimate and the calculation of thermal indices such as predicted mean vote (PMV), physiologically equivalent temperature (PET) and standard effective temperature (SET). The German VDI Guidelines 3789 Part II [87] (environmental meteorology, interactions between atmosphere and surfaces; calculation of short- and long-wave radiation) and VDI 3787 (environmental meteorology, methods for the human-biometeorological evaluation of climate and air quality for urban and regional planning. Part I: climate) [88] make up the base of the RayMan model. Experimental studies have been used to validate the tool [86].

2.2.2.6 SOLWEIG

The SOLWEIG (SOlar and Long-Wave Environmental Irradiance Geometry) model allows researchers to quantify the variations in the mean radiant temperatures (T_{mrt}) and PET in the urban environment spatially and temporally in the time horizon 2080–2099 [55].

3 Methodology

This section first describes the indices of human thermal comfort used in the case study cities, and then looks at the selected tools, metrics, spatial scales, scenarios and aims of each case study city.

3.1 Indices of human thermal comfort

On the meso and microscale, climatic parameters and conditions are mostly influenced by natural and artificial morphology. Their temporal and spatial behaviour are significant at different levels of regional and urban planning, i.e. design of urban parks or radiation conditions in urban canyons, and a variety of other applications [86,89,90].

The thermal component is an important factor, influenced by meteorological parameters such as air temperature, air humidity, wind velocity, mean radiant temperature and also short- and long-wave radiation [91,92]. These parameters thermo-physiologically affect human beings indoors and outdoors. For the estimation of thermal indices, common meteorological data is required.

3.1.1 Predicted mean vote and physiological equivalent temperature

Thermal indices, derived from the energy balance of the human body, are used in many applications of bioclimatology and applied climatology. In this deliverable, some of the analyses were conducted using the models in order to assess the human thermal experience in the urban environment.

The human thermal comfort level is measured by a number of biometeorological indices that associate microclimate conditions with human thermal sensation. These indices are categorized as steady-state models. Despite some research demonstrating that they cannot effectively account for the dynamic aspects of human thermal adaptation, thermal indices are still the most used in scientific literature [93]. Among the steady-state model studies, several have expressed thermal comfort using the PMV, an index that predicts average thermal response. In other studies, air temperature and thermal comfort in different design areas have been evaluated by means of the PET [51].

The PET is based on the Munich Energy-balance Model for Individuals (MEMI) [91], which models the thermal conditions of the human body in a physiologically relevant way. PET is defined as the physiological equivalent temperature at any given place (outdoors or indoors) and is equivalent to the air temperature at which, in a typical indoor setting, the heat balance of the human body is maintained with core and skin temperatures equal to those under the conditions being assessed. This way PET enables a layperson to compare the integral effects of complex thermal conditions outside with his or her own experience indoors [91]. Its calculation is influenced by the activity of the people, clothing and meteorological parameters such as wind speed and humidity.

It expresses the human thermal comfort in both indoor and outdoor environments using the international standard unit widely known as the Celsius degree (°C) [2]. It is easily comprehensible by all actors and professionals involved in the urban and design process, with any specific technical background. PET gives the measure of thermal comfort considering the meteorological parameters: air temperature, air humidity, wind velocity and radiation fluxes. It also takes into account the physics of the human body:

sex, height, activity, clothing resistance for heat transfer, short-wave albedo and long-wave emissivity of the surface [91] (Figure 2). In order to classify cold, neutral and heat stress in the urban canopies, the calculated values have been referred to the evaluation scale of Matzarakis and Mayer [94].

A brief description of the outputs is given below in order to provide the most relevant physical and technical aspects of their influence in human comfort and urban environment.

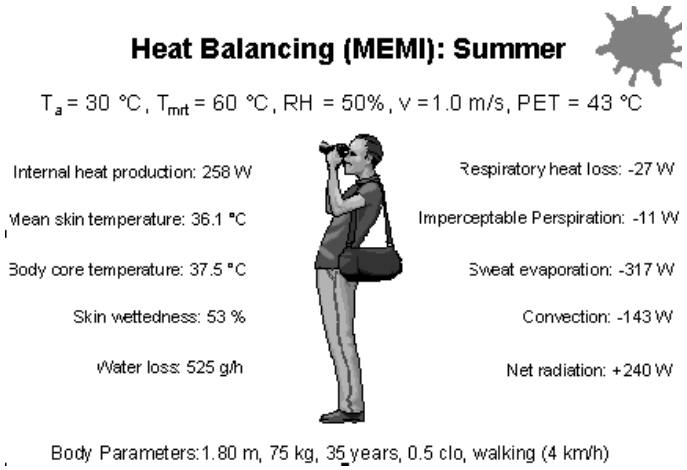

Figure 2 – Sample heat balance calculation with the MEMI for warm and sunny conditions [91].

Table 1 summarizes the level of thermal comfort that humans feel in the outdoor environment: all values will be classified following these ranges [94].

Table 1 – Ranges of the PET level corresponding to the thermal sensitivity and grade of physiological stress [92] [95] [96].

PMV (°C)	PET (°C)	Thermal perception	Grade of physiological stress
		Very cold	Extreme cold stress
–3.5	4		
		Cold	Strong cold stress
–2.5	8		
		Cool	Moderate cold stress
–1.5	13		
		Slightly cold	Slight cold stress
–0.5	18		
		Neutral	No thermal stress
0.5	23		
		Slightly warm	Slight heat stress
1.5	29		
		Warm	Moderate heat stress
2.5	35		
		Hot	Strong heat stress
3.5	41		
		Very hot	Extreme heat stress

PMV is expressed as a dimensionless quantity that scales between –4 (too cold) and +4 (too warm). Its values can be linked to the percentage of people that still feel comfortable at a given PMV value. The optimal value is 0, and at decreasing or increasing values, people increasingly feel uncomfortable. At a PMV value of 2, 80% of subjects complain, and towards a value of 4, nearly everyone feels uncomfortable.

PET and PMV depend on a number of additional meteorological variables including ambient temperature, relative humidity, wind speed and T_{mrt}. T_{mrt} is one of the most important indicators of human thermal comfort in order to obtain the human energy balance during summer conditions [97,98], with the greatest spatial variability within a microscale urban area due to complex geometry and heterogeneous surface characteristics.

3.1.2 Wet bulb globe temperature

Heat stress indicators such as the wet bulb globe temperature (WBGT) – which has been employed in deliverable D5.2 to estimate productivity loss associated with excessive heat stress – are very sensitive to LST as the latter determines the long-wave radiant heat load experienced by a person. The effect of vegetation on attenuating the WBGT should thus induce a beneficial impact for human exposure to heat stress.

3.1.3 Land surface temperature

LST is largely recognized as an indicator to assess the effects of surface radiative proprieties, energy exchange, internal climate of buildings and human comfort in the cities. LST is used in conjunction with other indicators, such as land-cover, land use, vegetation index and urban morphology [99,100,101,102].

For large domains such as cities, LST is typically determined by means of satellite remote sensing imagery. Recently, Oltra-Carrió et al. [103] conducted an investigation regarding the most suitable methods and algorithms to retrieve LST data from satellite thermal imagery. From this, it emerged that the temperature–emissivity separation (TES) algorithm [104] best reproduces urban surface temperatures. This algorithm does not require a priori knowledge regarding the emissivity of the surface, which is a definite advantage over urban areas as these are characterized by strongly deviating infrared emissivity values.

Currently, the ASTER instrument on board the EOS-TERRA satellite platform appears to be the sole instrument capable of employing this algorithm, as it is the only one with enough (five) thermal channels to actually apply it. ASTER imagery has a spatial resolution of 90 m in the thermal infrared part of the spectrum.

3.1.4 Normalized difference vegetation index

The normalized difference vegetation index (NDVI) is defined as:

$$NDVI = \frac{\rho_{nir} - \rho_{red}}{\rho_{nir} + \rho_{red}},$$

with $\rho_{red(nir)}$ representing the reflectance of the land surface in the red and near-infrared (nir) spectral bands. Live green vegetation generally exhibits much higher reflectance values in the near-infrared portion of the spectrum, so areas covered with vegetation would yield high NDVI values. The normalization achieved by dividing the reflectance difference by its sum is mainly intended to reduce atmospheric effects as much as possible.

3.2 Tools and selected metrics for the case study cities

This section provides an overview about the selected metrics and the fixed settings for each case study city analysed for this report.

Table 2 shows the methods and tools for doing the analyses, the conducted measurements and simulations, the indices used, and the analysed scenarios for the case study cities at the mesoscale, while Table 3 shows the same at the micro-scale.

Furthermore, all the specifications about the spatial and temporal scales are listed below.

Table 2 – Selected metrics and fixed settings for the case study cities analysed at the mesoscale.

City	Spatial scale	Model/tools	Index	Scenarios	Aim	Temporal scale or other comments
Antwerp	Mesoscale	Satellite thermal image	LST	The best satellite image (least contaminated by cloud) was selected for analysis.	Map the surface UHI (SUHI). Analyse the effects of green infrastructure on LST.	24 July 2012 at 12:57 local time, registered using the ASTER instrument.
		Land-use change experiments/UrbClim	Average daily mean, maximum and minimum temperatures. Annual mean number of heat wave days (HWDs).	The expansion of the urban areas and the implementation of green areas in the city core in current and future climate conditions.	Assess: The impact of different land-cover categories, in particular those involving urban vegetation; The UHI magnitude; and The number of HWDs.	20-year periods (1986–2005 and 2081–2100) on the average daily mean, maximum and minimum temperatures for the summer period (June–August).
		UrbClim	LST	The reference situation, using the actually observed vegetation fraction cover patterns (the vegetation within the urban core on average reaches around 20–30%). Subsequently, the same simulation was run, changing the amount of urban vegetation by setting a lower limit of 60%.	Assess the impact of city-wide vegetation abundance of UHI intensity. Describe and analyse the impact of land-cover changes, in particular those related to changes in the amount of vegetation, on simulated air temperature patterns. Set limits to what can be maximally achieved by greening the city.	Note that the analysis focuses on night-time (midnight) temperatures as (1) the UHI effect is strongest at night, and (2) there are indications that nocturnal temperatures, even though lower than daytime values, are more determinant when it comes to the impact on human health.
Paris	Mesoscale	UrbClim	LST	A simulation for the larger Paris area was done using the prognostic urban climate model.	Investigate the UHI intensity of an urban park zone versus the nearby built-up areas.	Period from 1st May to 30th September 2003.
Delhi	Mesoscale	Land-cover categories contained in the World Urban Database and Access Portal Tools. MODIS instrument on board the TERRA platform.	LST, NDVI and WBGT	The NDVI and LST were observed as an average for the measured month (February 2015).	Review the impact of vegetation abundance.	February 2015

Table 3 – Selected metrics and fixed settings for the case study cities analysed at the microscale.

City	Spatial scale	Model/tools	Index	Scenarios	Aim	Temporal scale or other comments
Antwerp	Microscale	In-situ measurements	Air temperature and number of nights exceeding the 18°C and 20°C nocturnal thresholds	One station was installed in the centre of the city, one at a rural location near Antwerp, and a third one in the city's main centrally located park, called the Stadspark.	Assess the benefit of urban greening on thermal comfort in urban environment.	The data was acquired during the summer of 2013 (from 10th July to 11th September).
		Mobile measurements	Air temperature	The car was driven along a trajectory starting at the bio farm (rural) station at 19:17, and crossing the entire city up to the harbour area (arrival there at 20:21), passing near the Stadspark in the process.	Measure the daytime maximum air temperature along the designed path.	Car equipped with a number of sensors, including actively and passively ventilated temperature sensors. The measurements were acquired during the afternoon and evening of 4th September 2013.
		ENVI-met	PMV	The simulation experiments were conducted on the Groenplaats city square.	Investigate alternative spatial designs involving additional green infrastructure.	Heat stress was calculated on 24th July 2012.
Bilbao	Microscale	ENVI-met	PET	Initial scenario, different ground materials and greening scenarios using grass, tree-lined streets.	Comparative analysis of green actions to improve outdoor thermal comfort inside typical urban street canyons.	The evaluation was performed in three urban street canyons characterized by different aspect ratios: a height/width (H/W) ratio of 1.3 "compact low-rise" exemplified by Casco Viejo, H/W 1.5 "compact mid-rise" exemplified by Abando/Indautxu, and H/W 3.5 "open-set high-rise" exemplified by Txurdinaga. The analysed scenarios were run on 6th and 7th August in order to simulate typical summer day conditions in Bilbao.
				Different orientation and greening strategies maintaining the following constant ratios: H_{tree}/H_{canyon} and W_{tree}/W_{canyon}.	Generalization of the first part of the work analysing the effects of orientation, aspect ratio, ground surface material and vegetation elements on thermal stress inside typical urban canyons.	

4 Results and discussion

This chapter presents the results of the climate analyses for the different case study cities: Antwerp, Paris and Delhi at the mesoscale and Antwerp and Bilbao at the microscale. VITO researchers worked on the cities of Antwerp, Paris and Delhi, while the analyses on the city of Bilbao were conducted by NTNU/TECNALIA. It should be noted that the latter, i.e. the Antwerp/Bilbao microscale case studies, were conducted in close cooperation with the respective municipal administrations.

4.1 Mesoscale case study cities

At the agglomeration scale, first an analysis of thermal satellite imagery on Antwerp was conducted to assess the effect of urban green areas on observed LST. Subsequently, the UrbClim model was run using different land-cover configurations, and an assessment was made of the impact of these different configurations on 2-m air temperature fields. Simulations were also conducted for the Paris area, where the effect of vegetation abundance on simulated temperature fields was assessed by means of a local statistical regression of simulated temperatures with respect to vegetation abundance. Finally, an analysis was done on the relationship between remotely sensed LST and vegetation abundance for the city of Delhi.

4.1.1 Antwerp

The next sections present the mesoscale analyses for the city of Antwerp.

4.1.1.1 Satellite thermal image

The SUHI was mapped by means of thermal infrared satellite imagery, and analysed for the effects of green infrastructure on LST.

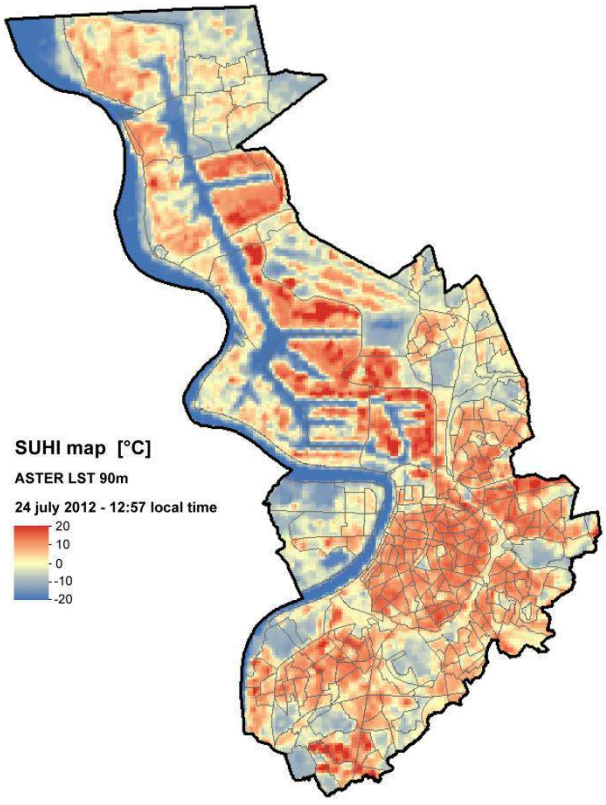

Figure 3 – LST for the Antwerp area on 24 July 2012 at 12:57 local time, as registered by the ASTER instrument. Note that LST is expressed with respect to the average value occurring in the image, i.e. the map shows temperature differences.

The relationship between the LST and the features of the urban surface cover was investigated. Care should be taken not to confuse air and surface temperature. The latter is the kinetic temperature of the surface of the materials making up the urban fabric, as seen by a sensor (satellite or otherwise) that captures radiation emitted by the surface. Typically, the SUHI exhibits a very strong pattern during the day, with values that may reach 50°C or more over certain surfaces, and thus can contribute strongly to the radiant heat load experienced by humans.

Through the Earth Remote Sensing Data Analysis Center (ERSDAC), a number of cloud-free images acquired during the summer were selected. Only daytime images were found, which is unfortunately somewhat limiting. The best satellite image (least contaminated by cloud) was then selected for analysis. This image is identified as "ASTL1A 12072410572012072502 94 51.3988 4.5116 2012-07-24T10:57:20Z", which includes the latitude and longitude of the centre of the image in decimal degrees. The date is 24 July 2013, and time information (last part of the identifier) is given in UT, whereby 10:57 UT corresponds to 12:57 local time.

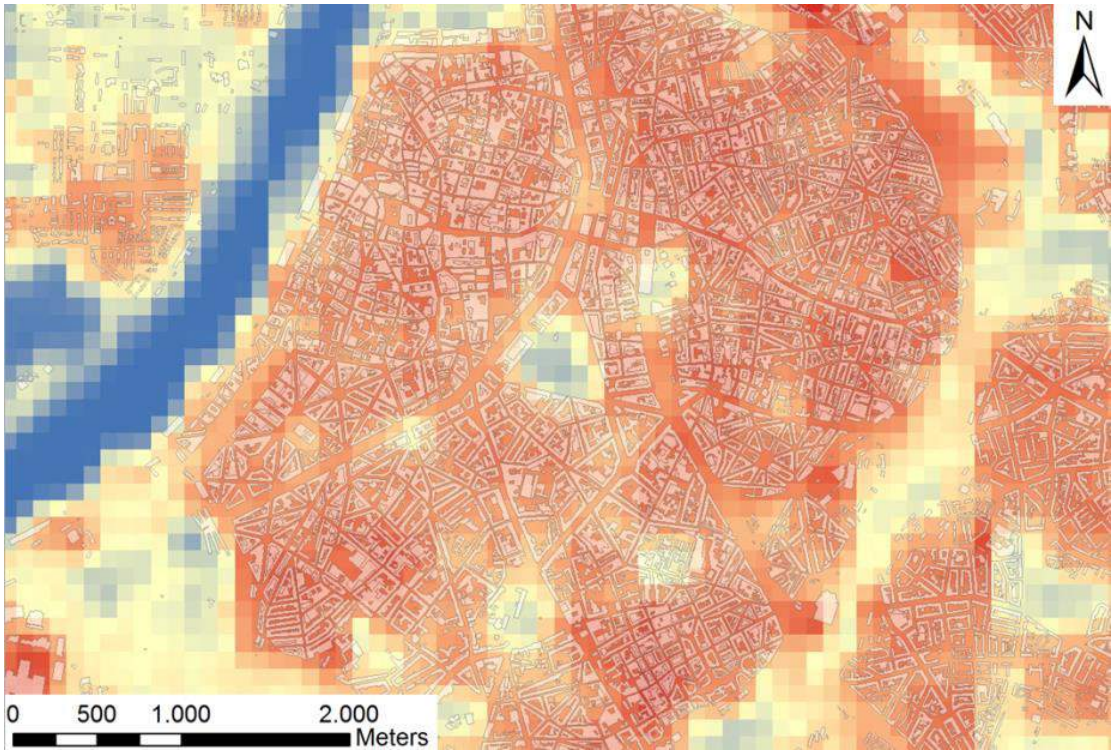

Figure 4 – Detail of the surface temperature map shown above for 24 July 2012.

Figure 3 shows the ASTER LST image. The heat island effect of Antwerp is clearly present in the image, the city being warmer by several tens of °C compared to the rural surroundings, which are mostly covered by vegetation. The harbour area also stands out distinctly as a local hotspot. The concerned areas consist mainly of large, open industrial terrain, with large asphalt or concrete surfaces, and roofs covered by dark roofing material, all elements that contribute to higher LST values. However, within the urban core of Antwerp, near the centre, a triangular area characterized by lower temperatures can be identified (Figure 4) at the position of the Stadspark (the major urban park in central Antwerp).

Figure 5 shows the LST data extracted from the satellite image over a transect including values for the Stadspark. This graph was constructed based on two different ASTER thermal satellite images, showing a high degree of consistency between both images.

From this image, it becomes clear that the LST values in the park are up to 15–20°C cooler than in the surrounding densely built-up areas.

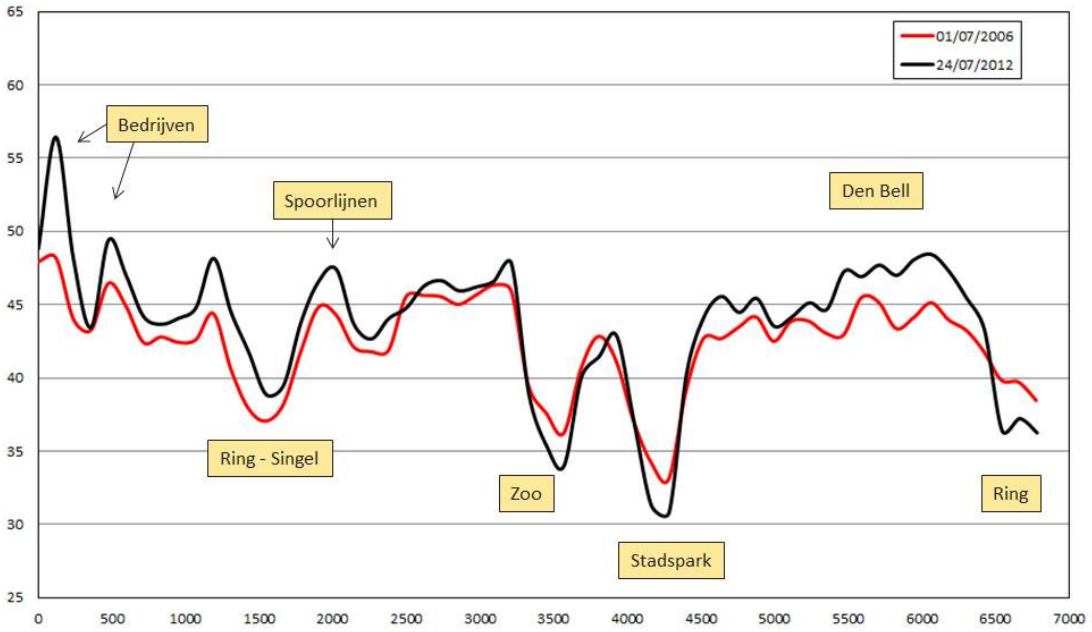

Figure 5 – LST values from a transect through the city of Antwerp from south-west to north-east, crossing the Stadspark. The black and red lines correspond to different satellite images.

4.1.1.2 Land-use change experiments

A series of localized land-use change scenarios was run with the UrbClim model for Antwerp in order to assess the impact of different land-cover categories, in particular those involving urban vegetation, on the UHI magnitude and the number of HWDs, both for current and future climate conditions.

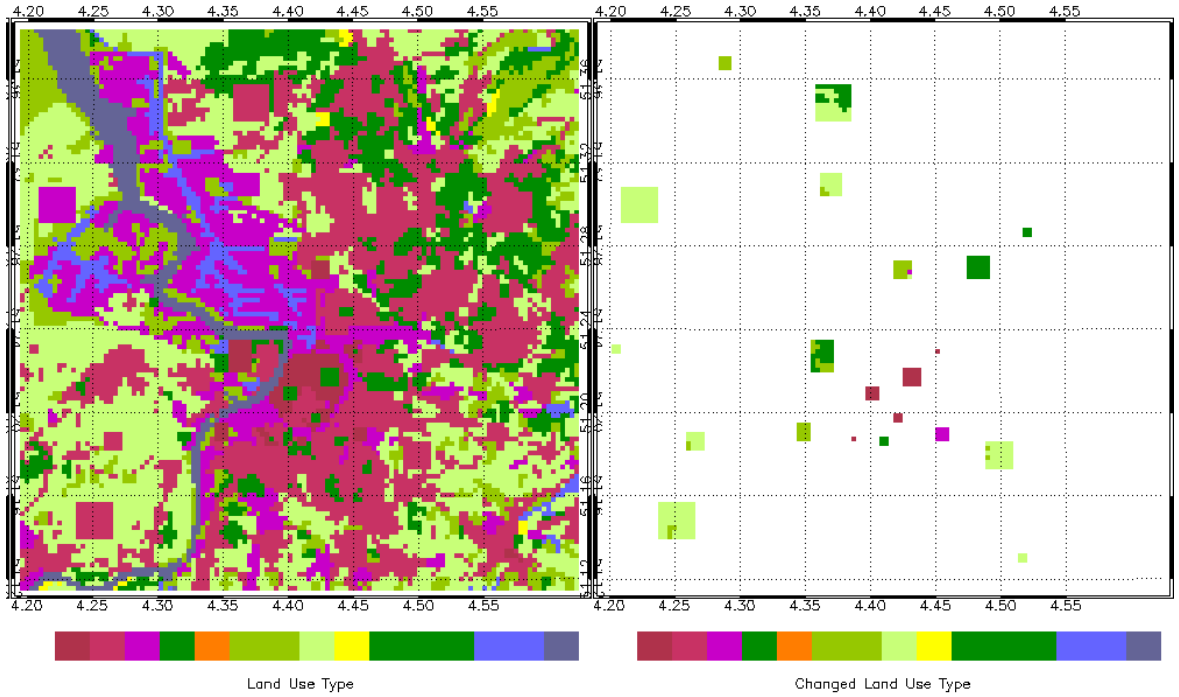

Figure 6 – The land-use scenario map of Antwerp (left) and the location's original land-use types of the changed areas (right). The reddish colours correspond to urban land use, dark green is used for forest and urban park vegetation, bright green for agricultural land (crops and pasture), and blue for water.

Since the city of Antwerp is mainly concerned with the expansion of the urban areas and the implementation of green areas in the city core, the scenario was limited to these particular changes.

The resulting land-cover change scenario maps (Figure 6) show the location of the changed areas, which include large and small changes distributed over the area, both close to and far from the city centre. New urban, suburban and industrial areas are added. Urban greening is limited to the city centre itself, where small to large parks have been added. Of course, land use is only one of the input parameters, and the new areas need values for the other parameters as well. Instead of using only one typical value per land-use type, VITO's researchers opted to give each changed grid cell the parameters of a randomly chosen grid cell from the corresponding land-use type. In this way, the changed areas have a realistic range of parameter values, from which many statistics can be obtained. The drawback of this method is that the result looks a bit spotty, especially for the vegetation cover and soil sealing.

Firstly, the impact from land-use changes in the UrbClim model has been assessed. This was done by considering the effect of the changes over 20-year periods (1986–2005 and 2081–2100) on the average daily mean, maximum and minimum temperatures for the summer period (June–August), as well as on the annual mean number of HWDs, a good indicator for changes in the extreme values.

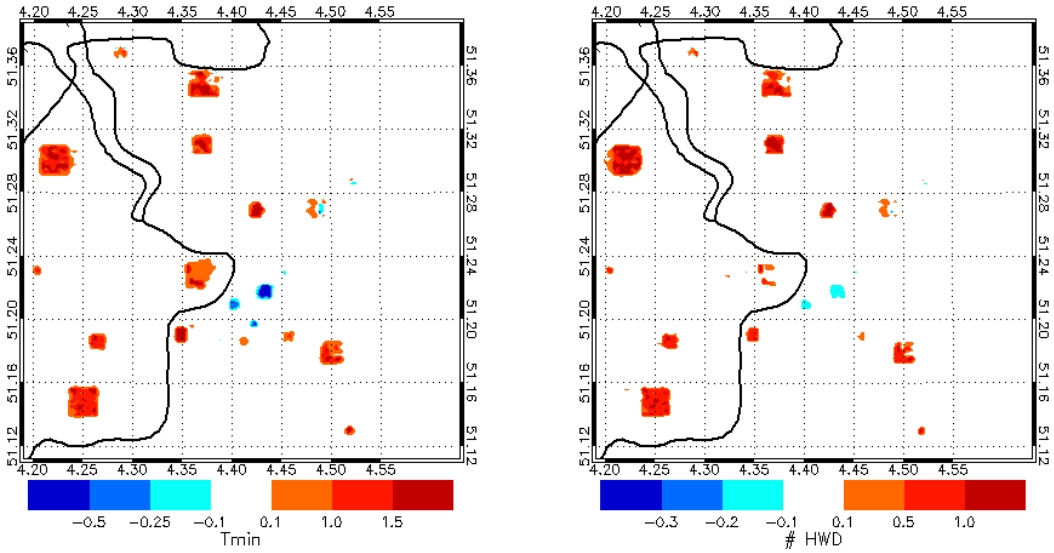

Figure 7 – Differences between the reference situation and the scenario for the period 1986–2005 for the average daily minimum temperature (left) and average daily maximum temperature (right).

Figure 7 and Figure 8 show the difference between the reference and the land-use change scenario simulated for the periods 1986–2005 and 2081–2100.

It is clear from these figures that, when considering averages, the effects are limited to the location of the land-use changes, and do not have an impact on the wider environment. Furthermore, the magnitude of the effect is rather limited, with mean temperature changes up to 1.5°C for large urbanized areas and –0.4°C for parks.

The effect is larger (up to 2°C and –0.5°C) for the daily minimum temperatures. It should be kept in mind that the mean night-time UHI intensity of Antwerp city centre is around 3°C, so in that regard the changes are certainly not negligible. The impact on the number of HWDs is comparable, with changes up to 1.5 and –0.3 days, as compared to average city centre HWD values of around 2.

Regarding the simulations of future conditions, the effect of the land-use changes on the average temperature values is almost exactly the same as for the current period (so is the UHI). The effect on the number of HWDs is much larger, but the projected number of HWDs for the city centre at the end of the century rises to around 20, so the relative effect is comparable to that of the present day.

In conclusion, urbanization has an effect of up to 2°C on the average temperatures in UrbClim, which is consistent with reported measurement and modelling studies. This may not seem much, but it is significant with respect to the average UHI effect of around 3°C. The construction of (large) parks in the city centre brings local cooling of up to 0.5°C, which is lower than what is reported in the literature (effects up to 1.5°C) and further demonstrates the need to include shading effects in UrbClim in order to highlight the benefits of green infrastructure.

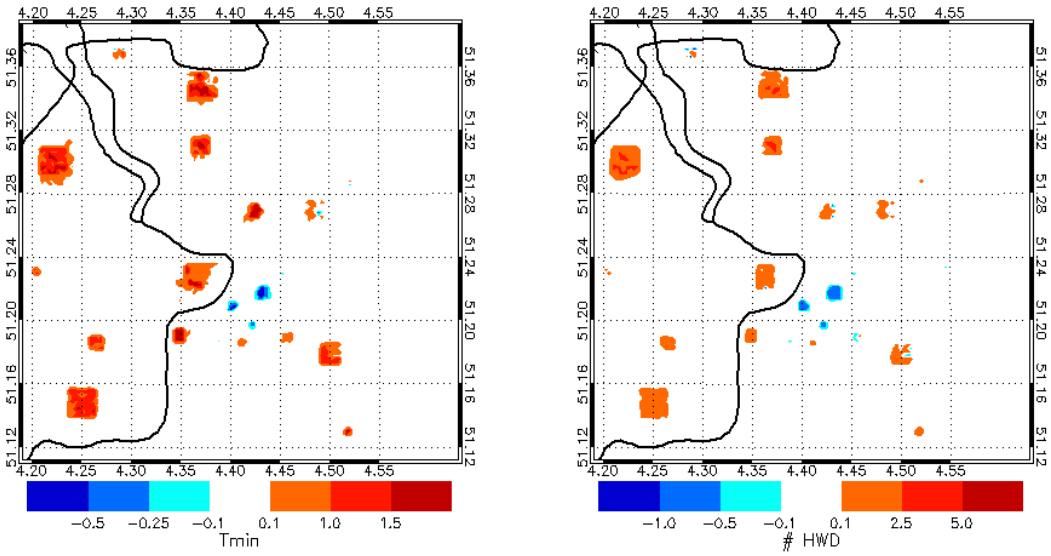

Figure 8 – Differences between the reference situation and the scenario for the period 2081–2100, based on the full set of General Circulation Model (GCM) simulations.

Initially, the idea was to look for simple relations between the amount of soil sealing and/or vegetation cover change and the corresponding temperature effect, which could be useful to generate rule-of-thumb estimates. Unfortunately, clear associations could not be obtained; correlations were found to be low. However, when also considering the initial land-cover types, an interesting effect became apparent: in areas characterized by a low roughness length (grassland and cropland), much larger temperature effects can be expected than in areas with higher roughness lengths (forests and urban parks).

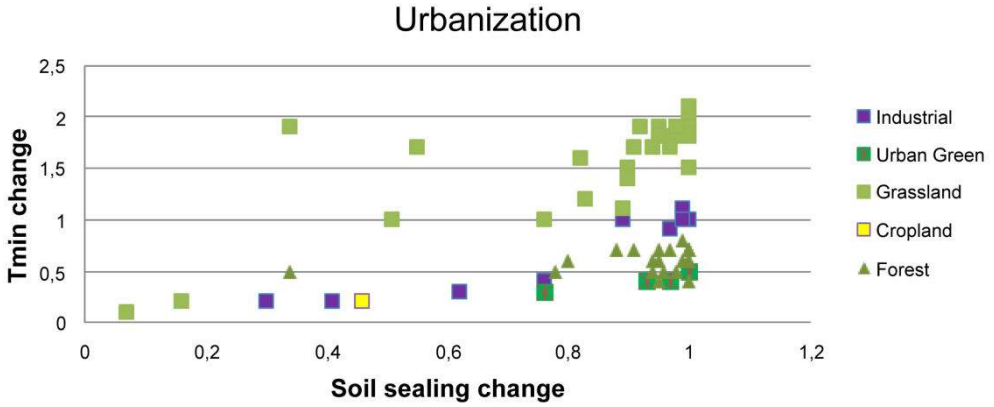

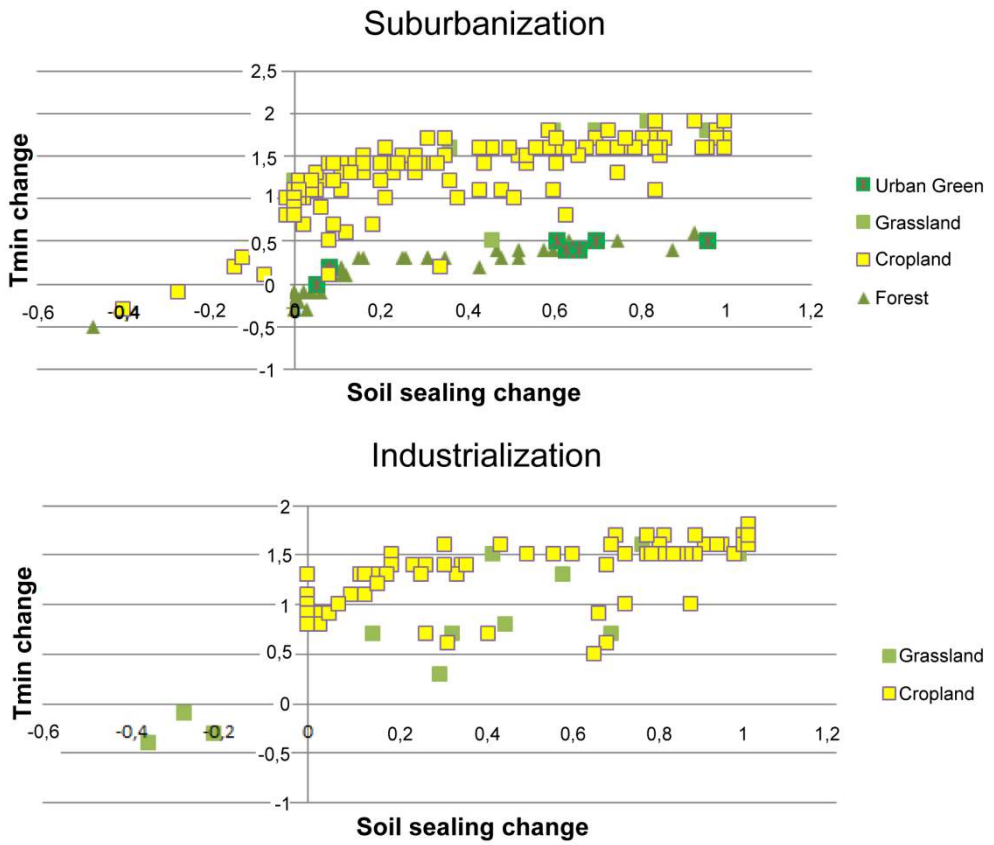

Figure 9 – Relation between the change in soil sealing and the daily minimum temperature for the three types of urbanization, classified according to the original land-use type.

When considering Figure 9, it would appear that the type of urbanization (conversion to dense urban, suburban or industrial land use) does not matter much for the maximum temperature reduction effects that can be achieved within each original land-use class. Therefore, and in order to have a larger number of data points, all the urbanization data is taken together to define the relationships.

In Figure 10 and Figure 11, the relation between the temperature effect and changes in soil sealing or vegetation cover are explored for each initial land-use class.

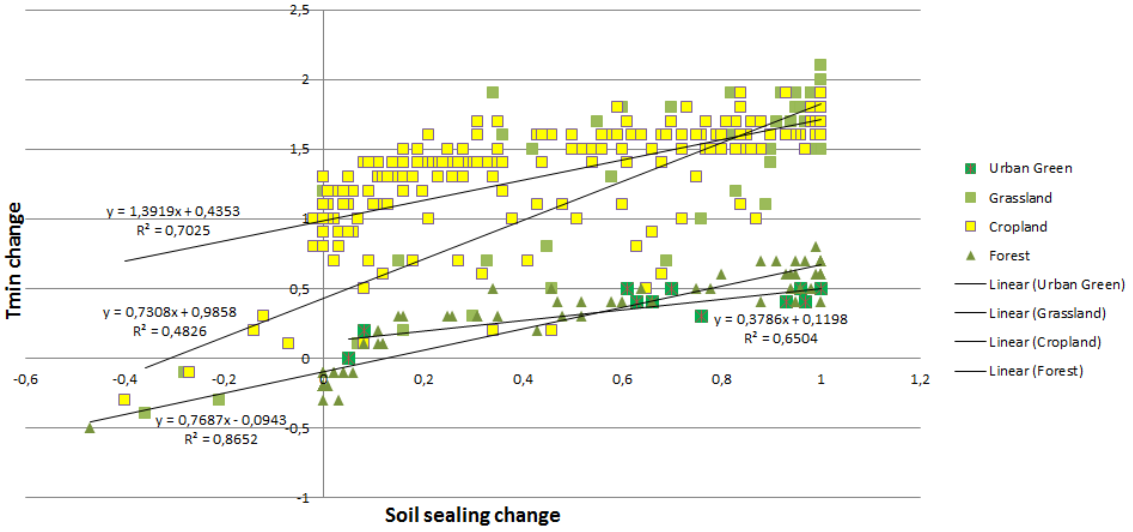

Figure 10 – Total urbanization – relation between the change in soil sealing and the daily minimum temperature for all urbanized grid cells, classified according to the original land-use type.

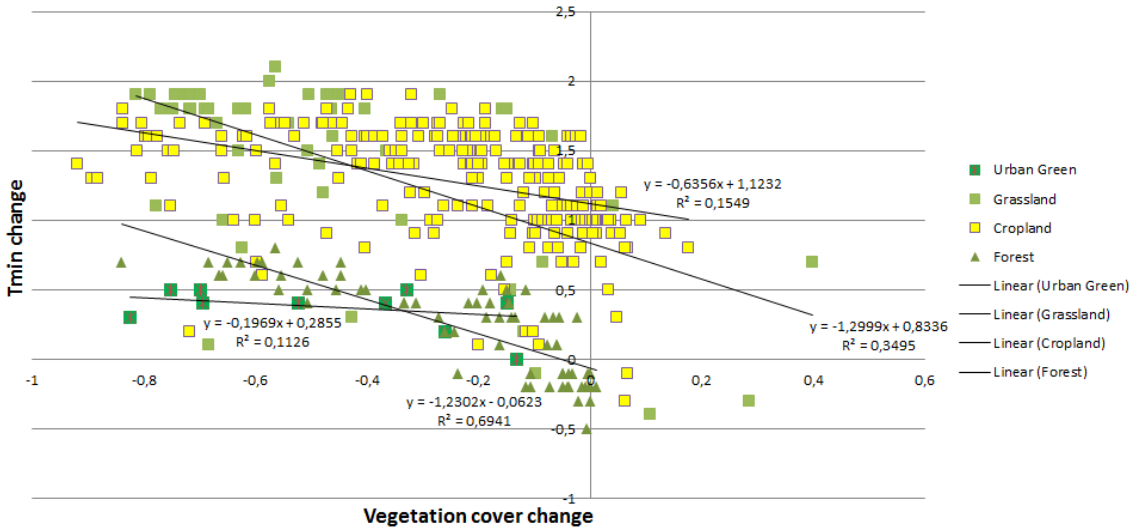

Figure 11 – Total urbanization – relation between the change in vegetation cover and the daily minimum temperature for all urbanized grid cells, classified according to the original land-use type.

The coefficients of determination are relatively high, especially for the soil sealing changes, which means these relations are robust and could be used to quickly estimate the expected effect of land-use changes. This data can be built upon by adding more from other land-use change scenarios, and comparisons between the different cities can be made. Finally, a similar experiment was done for the conversion of the urban area to urban green (Figure 12). However, in order to keep the change scenarios realistic, the number of resulting data points was necessarily limited, which led to relations with a smaller coefficient of determination.

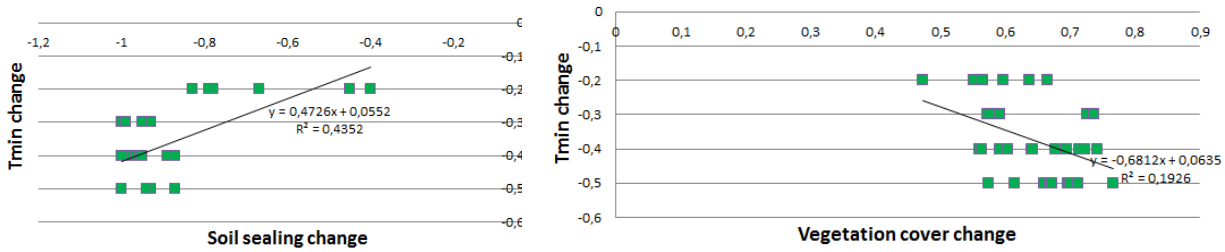

Figure 12 – Greening – relation between the change in soil sealing (left) or vegetation cover (right) and the daily minimum temperature for all greened grid cells.

In conclusion, this experiment enables the evaluation of whether a large park has an additional temperature effect compared to a small park, as parks were created with different surface area sizes and comparable changes in land-cover (all from dense urban to urban green) and vegetation cover (all grid cells from nearly 0% to almost 100%).

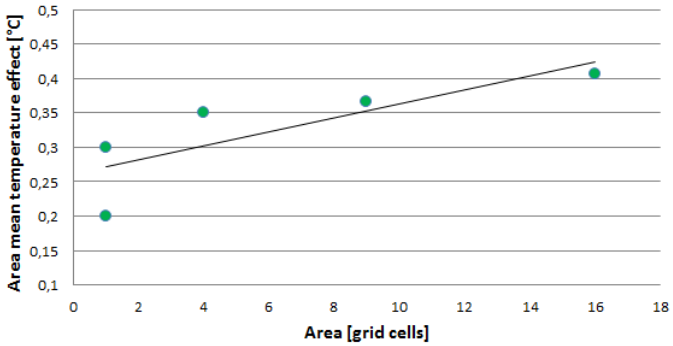

Figure 13 – Adding urban green – relation between the area surface size of new urban green and the area mean effect on the daily minimum temperature.

When calculating the area mean temperature effect for all parks (Figure 13), it is clear that the large park (1 km²) creates an additional cooling effect of 0.1°C compared to the small parks (0.06 km²). This means that when cities envisage optimal city-wide cooling results, it is better to create one big park than several small ones.

Most probably the same is true for urbanized areas (i.e. enhanced warming effect in large urbanization projects), but since the urbanized areas are too heterogeneous regarding their original land-cover and vegetation and soil sealing changes, this cannot be evaluated.

4.1.1.3 Impact of city-wide vegetation abundance of UHI intensity modelling with UrbClim

This section describes an analysis of the impact of land-cover changes, in particular those related to changes in the amount of vegetation, on simulated air temperature patterns.

A sensitivity study was conducted, considering overall vegetation abundance in the city as a driver, taking Antwerp during the summer of 2011 as a study case. This study first considered the reference situation, using the actually observed vegetation fraction cover patterns (obtained from a satellite vegetation index). Subsequently, the same simulation was run, changing the amount of urban vegetation by setting a lower limit of 60% on the vegetation cover occurring in the domain.

It should be noted that this is a rather drastic change compared to the reference situation, in which the vegetation within the urban core on average reaches around 20–30%. However, the goal of this exercise is not to evaluate a realistic adaptation measure, but rather to set limits to what can be maximally achieved by greening the city. Note that the analysis focuses on night-time (midnight) temperatures as (1) the UHI effect is strongest at night, and (2) there are indications that nocturnal temperatures, even though lower than daytime values, are more determinant when it comes to the impact on human health [5].

Figure 14, presents the results from this sensitivity study, showing that an increase from approximately 20–30% to 60% vegetation cover in the city lowers the temperatures by around 0.6°C (from 18.5°C to a bit less than 18°C). This may appear low, given that the "total" UHI intensity amounts to about 2.5°C (difference between the urban value of around 18.5°C and the rural darkish blue of approximately 16°C), and one would hope that increasing vegetation from 20–30% to 60% would lead to a larger temperature benefit.

However, one should keep in mind the roughness effect. Indeed, while the cooler rural areas (blue colours) exhibit temperature values of around 16°C, the rural forest areas around the city reach 17°C (yellow-green). In relation to this, the drop in temperature of 0.6°C brought about by a relative change in vegetation of 30% (from 30% to 60%) is rather consistent. The reason why the forested areas are comparatively warm at night (compared to e.g. grassland areas) is that over rough surfaces, vertical mixing is enhanced so that night-time temperatures do not descend as low as over flat and smooth areas.

As a conclusion to this exercise, it is fair to say that greening the city does have an impact, but to a limited extent only, as the city's roughness limits nocturnal cooling.

Consequently, it is not possible to achieve a very large reduction in the UHI intensity, unless the urban roughness length is also reduced.

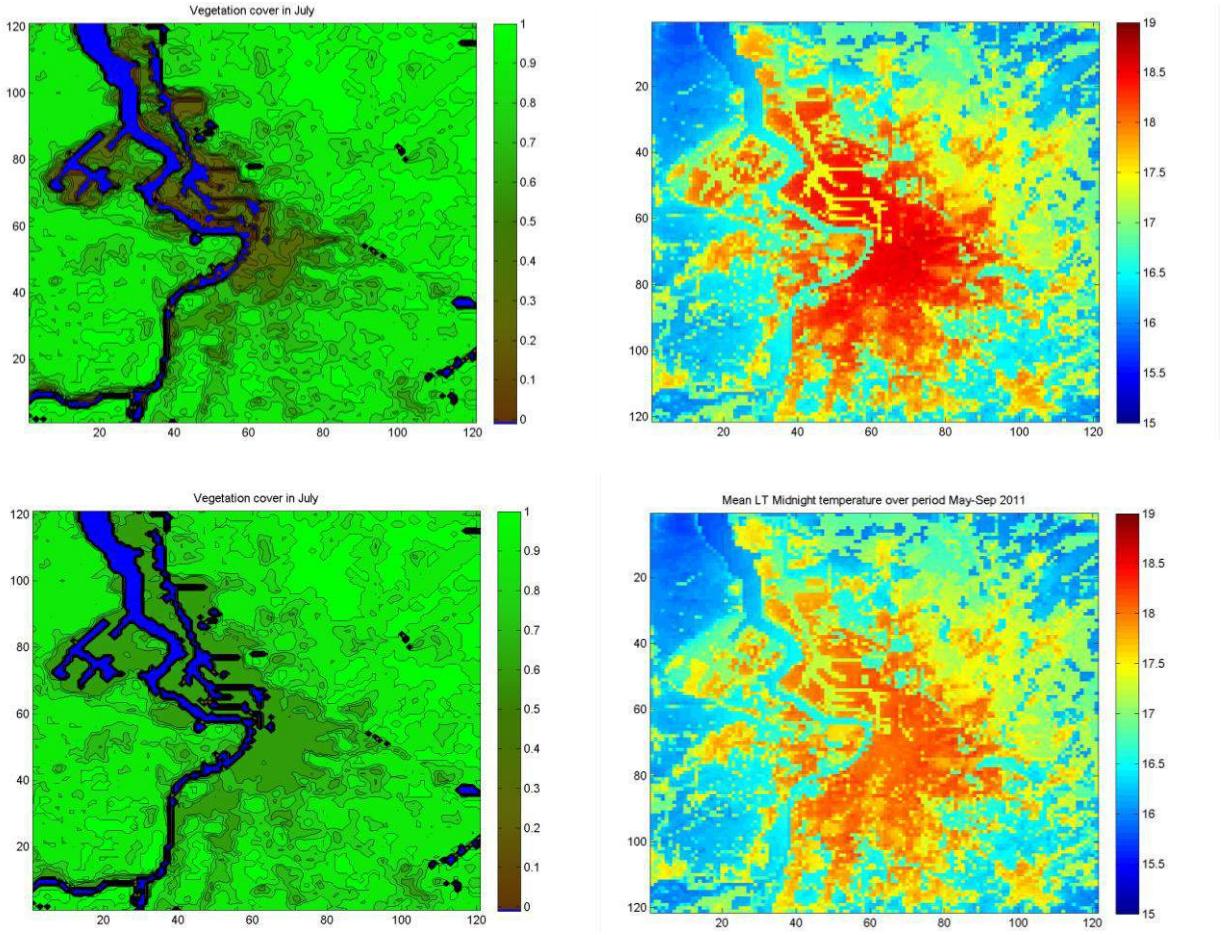

Figure 14 – Vegetation cover for July (left) and average midnight temperature in the period May–September 2011 (right), for the reference situation (upper panels) and for a situation with enhanced urban vegetation (lower panels).

Of course, an important caveat is to be accounted for here. Indeed, by only considering *air temperature* in the characterization of the UHI intensity, certain impacts of vegetation on heat stress, such as the fact that vegetation creates a shadow during the daytime, were ignored, thus contributing to reduced human exposure to heat. However, to account for such effects would require the use of detailed 3D urban canopy models, which are fraught with other types of limitations, such as their inability to cover the whole city (computational restrictions generally limit the use of such models to domain sizes of a city quarter at best).

Elsewhere in this report, such high-resolution models that also account for radiative effects are used to investigate these effects in more detail.

4.1.2 Paris

The next sections present the mesoscale analyses for the city of Paris.

4.1.2.1 Regression-based sensitivity analysis modelling with UrbClim: air temperature versus green areas

This section looks at the UHI intensity of an urban park zone versus the nearby built-up areas. This analysis was done for the area of Paris (France), using both in-situ measurements and modelling results for the (extended) summer (May–September) of 2003. This particular period is characterized by a wide range in temperature conditions, with daytime maximum temperatures in the area as low as 12°C on some days in May,

and reaching just short of 40°C on the hottest days during the first half of August of that year.

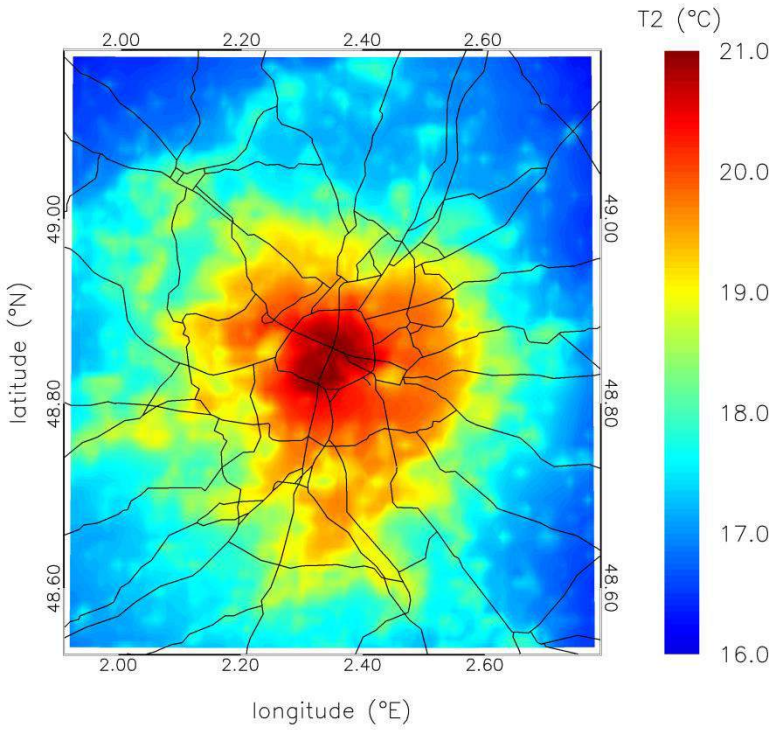

Figure 15 – Study domain centred on the city of Paris. The colour pattern shows the night-time (22:00 UT) 2-m temperature field averaged for the period May–September, as simulated by the model described in this section.

The observations used are synoptic meteorological data contained in the archives of the National Climatic Data Center (US), from which data was acquired for one urban and one rural location in the Paris region (see station positions in Figure 15). The Paris-Montsouris station (WMO code 071560) is taken as representative for urban climate conditions. It is located at approximately 48.81°N and 2.33°W, which is inside Montsouris Park near the centre of Paris. This roughly square park measures approximately 400 m on a side, and the station is positioned within the park more than 100 m from the nearest edge. Therefore, the representability of this location for urban conditions is to be taken with caution. The Melun-Villaroche station (WMO code 071530) is located at a position of 48.61°N and 2.68°W, which is near a small airfield 8.5 km north of the centre of Melun, which itself is 35 km from the city centre and 20 km from the outskirts of Paris. It is located in the middle of agricultural fields and grassland, several kilometres from the nearest human settlement, thus constituting a representative rural station.

The analysis conducted here is based on hourly 2-m air temperature observed at both stations during the period 1 May to 30 September 2003. Based on this data, a time series of hourly UHI intensity by taking the temperature value of Paris minus that of Melun have been constructed. While the observations from the two stations yield relevant insights, they obviously contain limited spatial information. More importantly, the station used for urban conditions is limited in its representation of the UHI intensity of Paris as it is located inside a park. Given the well-known cooling properties of urban green areas, this presumably underestimates the actual UHI intensity in the city's built-up zones. Therefore, it is necessary to look towards numerical modelling to complement the observation-based results described above.

A simulation for the larger Paris area for the period May–September 2003 was conducted using the prognostic urban climate model described in [105]. This model is composed of

a surface energy balance scheme coupled to an atmospheric boundary layer model [78]. The approach is a prognostic one, i.e. starting from an initial state, the model calculates subsequent temperature fields for soil, vegetation and urban substrate, and the overlying air. The main outcome consists of hourly raster files containing relevant climatic quantities such as 2-m air temperature. A particular aspect of this model is that the surface energy balance scheme is constrained through a data assimilation procedure, which uses remotely sensed thermal infrared imagery together with a so-called particle filter (sequential Monte Carlo) approach [106]. The remote sensing infrared imagery was taken from the MODIS archive containing LST values derived from 1-km brightness temperature imagery (both day- and night-time) acquired by the MODIS instruments on board the TERRA and AQUA satellite platforms. The raw imagery was corrected for atmospheric and surface emissivity effects, as described in [107]. The specification of the required terrain parameters is done based on digital raster files containing CORINE land-cover, distributed by the European Environment Agency. The spatial distribution of vegetation abundance is estimated using the MODIS NDVI. Large-scale meteorological conditions are accounted for by forcing the model with external fields of relevant quantities, such as temperature, wind speed vector components and humidity, from the ERA Interim archive of the European Centre for Medium-Range Weather Forecasting (ECMWF). Also, the initial soil temperature and volumetric moisture content are specified from this source.

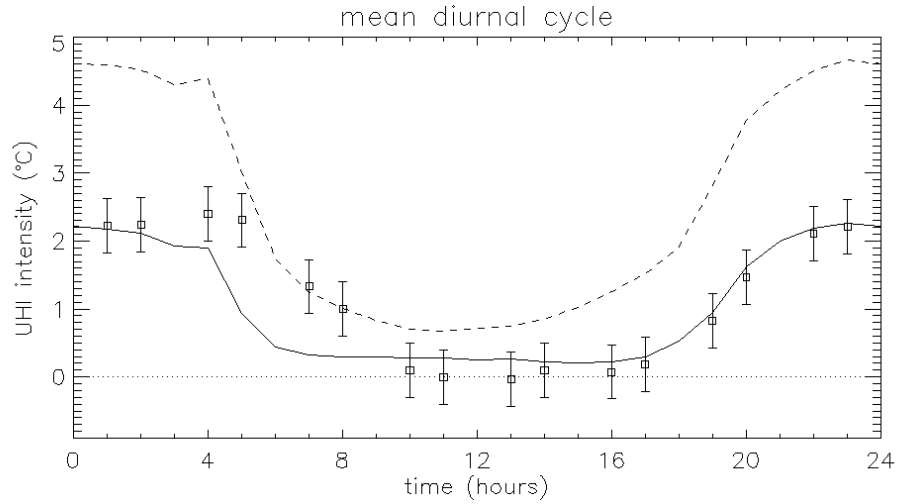

Figure 16 – Observed (symbols) and simulated (solid line) mean diurnal cycle of the UHI intensity between Paris-Montsouris (urban park) and Melun-Villaroche for the period May–September 2003. The dashed line shows the non-adjusted simulated value, which corresponds to fully urban conditions.

Downwelling short- and long-wave radiation, which is required as an input for the surface energy balance scheme, is specified from geostationary METEOSAT satellite imagery, which is distributed by the Land Surface Analysis Satellite Applications Facility (Land SAF) of Europäische Organisation für meteorologische Satelliten (EUMETSAT). Further details regarding the urban climate model, required input data and results of validation cases are available in [105,107,108].

The urban climate model was run for the wider Paris area, on a domain covering 100 km × 100 km, at a spatial resolution of 1 km. While this resolution is a constraint imposed by the spatial resolution of the MODIS 1-km satellite imagery, it would appear that for a large city such as Paris, this level of spatial detail is capable of providing an overall temperature pattern at the scale of the wider agglomeration.

Obviously, as in any model, the urban climate model relies on a series of simplifying assumptions. In order to create confidence in the simulation results, validation of 2-m air

temperature was conducted by comparing simulated values with observations from the two meteorological stations (Paris-Montsouris and Melun-Villaroche) described in the previous section. In fact, rather than validating the urban and rural temperatures separately, the validation concentrated on the urban–rural temperature increment, because this is the main interest here.

However, the spatial resolution (1 km) used in the modelling approach is problematic when it comes to comparing simulated temperatures with observed values. Indeed, as mentioned above, the urban observations were taken from a station located inside a park. Given the park's dimensions (around 400 m diameter), its surface area occupies only around 16% of a model grid cell, or less if it is located within different adjacent grid cells. In order to account for this discrepancy, a simple method was designed to adjust the simulated temperatures for the presence of vegetation so as to establish a better level of comparison with the observations done in the park.

For this method, hourly temperatures were simulated for the grid cells containing the positions of the two meteorological stations. For the urban station, the hourly simulated temperature of the eight surrounding grid cells was also extracted, thus yielding a total of nine simulated urban temperature values for each hour of the concerned period. With these temperatures, nine hourly UHI intensity time series were calculated by subtracting the concurrent rural values. For each individual hour, a regression was done between hourly UHI intensities and the percentage of impermeable surfaces, using the values for the nine neighbouring grid cells. The resulting regression coefficients were then employed to extrapolate the simulated central (i.e. at the urban station's position) UHI value to conditions of zero per cent impermeable surface, to mimic the conditions in the park.

These adjusted temperatures were averaged for each hour of the day for the whole period to yield a mean diurnal cycle for the period May–September 2003. Figure 16 shows the result obtained from the simulated and adjusted temperatures, together with the corresponding observed values. The magnitude of the error bars is 0.4°C, which is a value based on the intercomparison of nearly co-located thermometric measurements obtained at a few locations [78,109]. Error statistics were calculated for the simulated (against the observed) UHI intensity values, yielding a mean absolute error of 0.66°C, a correlation coefficient of 0.79, and a bias of –0.49°C.

More importantly, the mean diurnal UHI intensity representative of fully urban conditions was also calculated using the regression relations between the hourly UHI intensity and the abundance of impermeable surface in the neighbourhood of the urban station, but extrapolated towards a fully (hundred per cent) impermeable surface. The result is shown in Figure 16 as a dashed line, and the difference with the solid line is a measure for the effect of the park on the UHI cycle. This result reveals that, throughout most of the day, the park exhibits roughly half the UHI intensity of the surrounding dense urban zones, thus confirming the potential of urban green space as a relevant climate adaptation measure.

4.1.3 Delhi

The next section presents the mesoscale analysis for the city of Delhi.

4.1.3.1 The impact of vegetation abundance on land surface temperature

The effect of urban vegetation on remotely sensed LST for the city of Delhi was analysed. Figure 17 shows the land-cover layout of the wider Delhi area, based on the land-cover categories contained in the World Urban Database and Access Portal Tools (WUDAPT) classification (see www.wudapt.org).

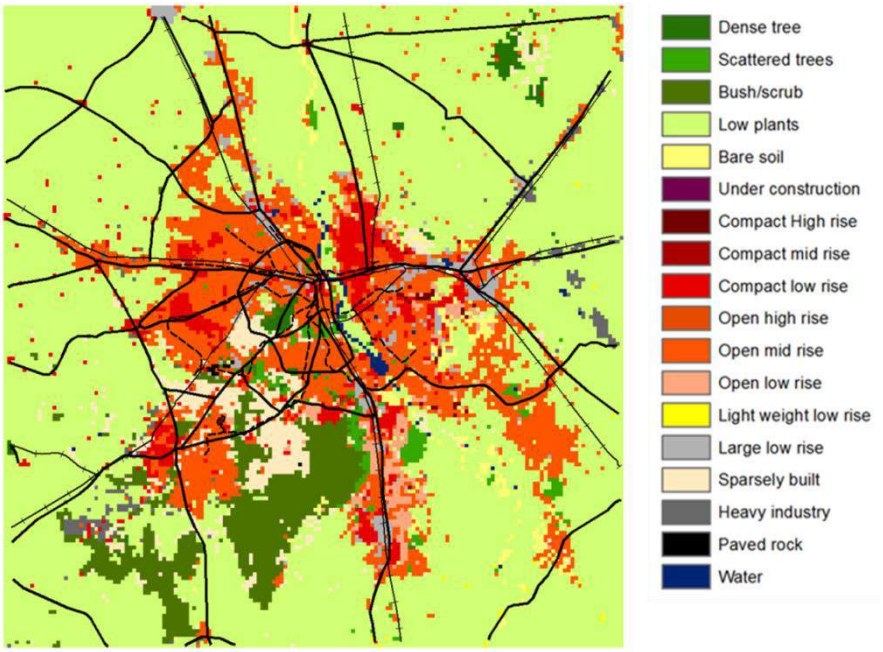

Figure 17 – Land-cover map for Delhi and surroundings, base year 2015. The land-cover categories are those of the WUDAPT classification.

The analysis is done based on two quantities, NDVI and LST.

Here, the NDVI based on reflectance by the MODIS instrument on board the TERRA platform was observed as an average for the month of February 2015. Figure 18 shows the NDVI patterns in the Delhi area, with low values over the city and higher values (i.e. more vegetation) around the city.

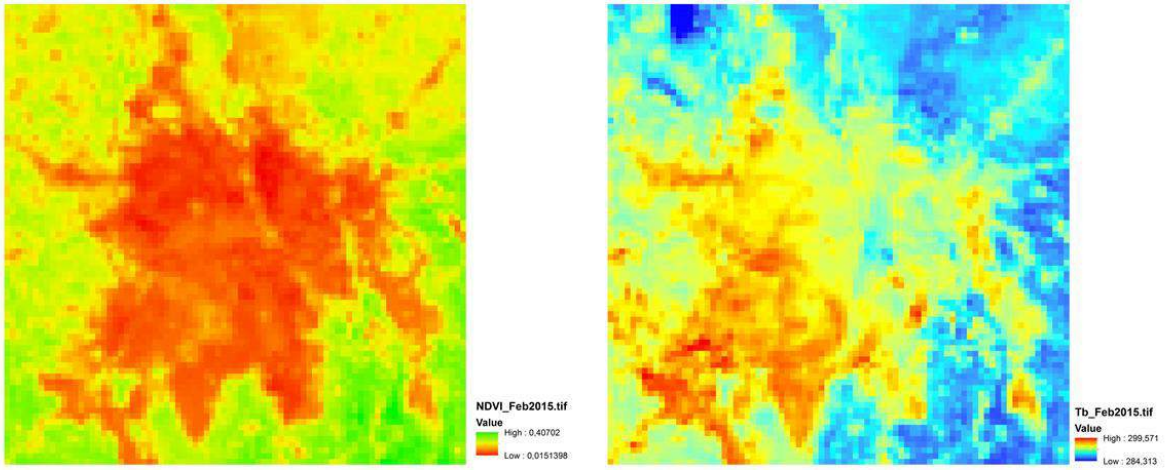

Figure 18 – Average NDVI (left) and LST (right) for the Delhi area, February 2015.

The LST used here is also taken from MODIS-TERRA imagery. It actually employs the so-called top-of-atmosphere brightness temperature, which yields an underestimation of the actual LST as well as of the actual temperature range, but otherwise it is a relevant indicator of surface temperature.

Figure 18 is the LST map for February 2015, and it immediately shows that the urban portions of the domain exhibit higher LST values.

From the NDVI/LST pair of images it is immediately clear that an inverse relation exists between the two, i.e. areas with sparse vegetation cover exhibit the higher temperatures,

and vice versa. This is visible even in smaller structures, such as in the quasi-linear feature extending in the upper-right corner of the images contained in Figure 18.

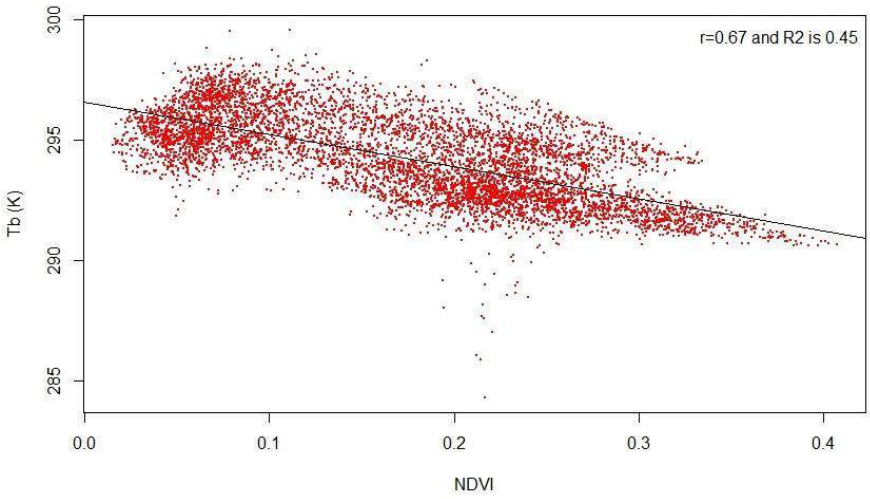

Figure 19 – Regression line between the observed LST (denoted Tb, in K) versus the NDVI for Delhi, February 2015.

The further analysis is straightforward: a regression line linking the LST linearly to the NDVI has been calculated, as shown in Figure 19.

This regression analysis quantitatively confirms the inverse relationship between both quantities, with a slope of around 5°C between the bare (NDVI = 0) and greener (NDVI ≈ 0.4) portions of the domain. The correlation between both quantities in the considered situation amounts to r = 0.67.

To end this section, it should be noted that the LST should not be mistaken for the air temperature.

In most results reported so far (e.g. deliverables D4.1, D4.2), air temperature has been used to characterize the UHI effect. Nevertheless, the LST is also a very relevant quantity that has a strong impact on the exposure of humans to heat stress.

4.2 Microscale case study cities

At the microscale, two case study cities, Antwerp and Bilbao, have been analysed by VITO and NTNU/TECNALIA respectively. The work was performed in collaboration with the respective municipal administrations.

4.2.1 Antwerp

For the city of Antwerp, a series of in-situ and mobile (car) measurements were conducted to provide evidence of the impact of urban green on temperature. This section presents the results of these measurements.

4.2.1.1 In-situ measurements

In order to assess the effect of urban green, several stations in and near Antwerp were used: one in the centre of the city, one at a rural location near Antwerp, and a third one in the city's main centrally located park, called the Stadspark.

For the in-situ measurements, an air temperature sensor of the highly accurate RTD type (PT1000) was used, housed in an actively ventilated radiation enclosure (43502 Aspirated Radiation Shield, Young Model type) (Figure 20).

RURAL: Bio farm at Vremde
51.16600833 N, 4.54864722 E
This station is located 10–15 km from the centre of Antwerp in the community of Vremde, in an open grassland area more than 150 m away from the nearest buildings.

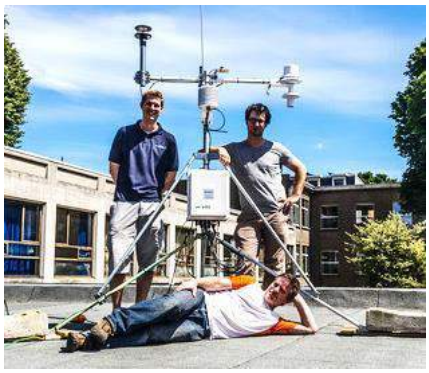

URBAN: Koninklijk Lyceum Antwerpen
51.208525 N, 4.41022778 E
Located on the roof of a minor building in a large school yard, 10 m from the nearest wall.

URBAN PARK: Stadspark
51.21164444 N, 4.412361111 E
This station was mounted in the Stadspark, south of the centre of the park, near a lake and surrounded by a mixture of grass and trees.

Figure 20 – The stations for the in-situ measurements in Antwerp.

Under maximum radiation exposure (1,000 Wm^{-2} incident solar radiation), the difference between air temperature in the enclosure and the ambient temperature is limited to a maximum of 0.2°C. All temperature measurements were done at a height of 1.8 m, but may commonly be referred to as "2-m air temperature".

The data, which was acquired during the summer of 2013 (from 10 July to 11 September) (Figure 21), was analysed with respect to the average diurnal cycle of the urban–rural temperature difference, using the data from the bio farm in Vremde as a baseline, i.e. the curves show the temperature for a given station minus the values recorded in Vremde.

The urban station exhibits the strongest average UHI intensities, with values below 1°C during the day and exceeding 3°C at night. The alleviating effect of the park is evident from the green curve (Stadspark): during the day, the UHI effect nearly vanishes, and during the night it is between 2°C and 2.5°C, i.e. slightly more than 1°C below the value recorded at the urban (Lyceum) station.

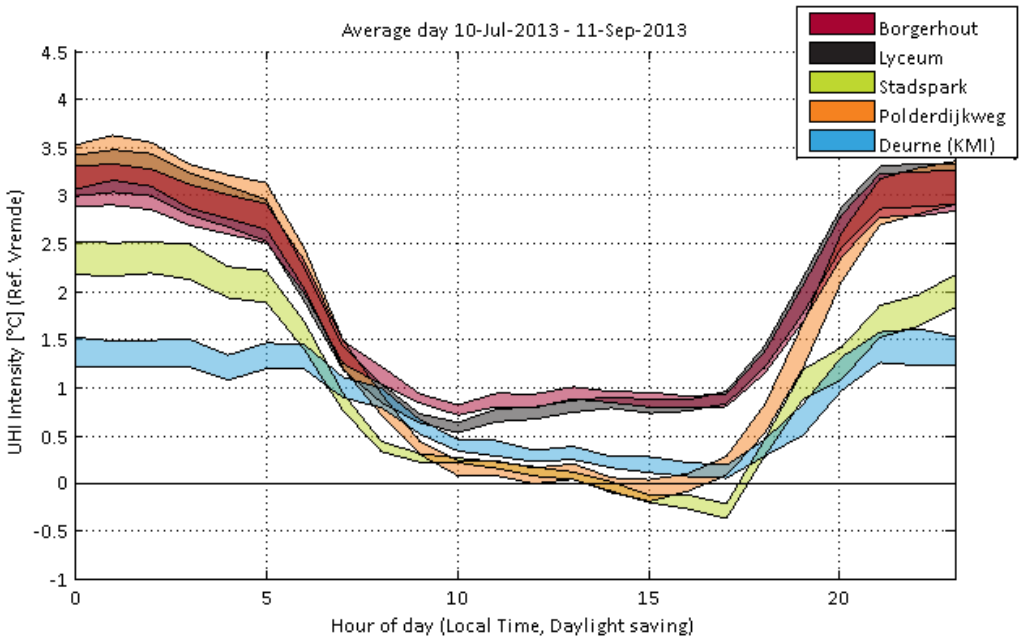

Figure 21 – Mean diurnal cycle of observed air temperature with respect to the rural station of Vremde. Borgerhout and Lyceum are central urban stations. Stadspark is a station in an urban park location, Polderdijkweg is in the harbour area, and Deurne (KMI) is at the local airport. For this review, we focus on the stations Lyceum (urban station) and Stadspark (urban park location). The width of the bands is a measure for the statistical uncertainty of the observations.

Another way of assessing these data, perhaps more relevant in the context of heat stress exposure estimates, is to consider the number of nights (out of the total of 63) during which the temperature did not drop below 18°C or 20°C.

The threshold of 18°C is related to the nocturnal minimum temperature used in the definition of a heat wave day in Belgium, and the second (20°C) is often referred to as that defining a "tropical night".

Table 4 – Mean UHI statistics for the urban and urban park stations, separately for daytime (10–18h local time) and night-time (22–4h). The two rightmost columns give the number of nights with minimum temperature values exceeding the thresholds of 18°C and 20°C respectively.

Station	Site type	UHI day mean (°C)	UHI night mean (°C)	# nights T_{min} > Tmin>18°C	# nights T_{min} > Tmin>20°C
Lyceum	urban	0.74	2.94	13	6
Stadspark	urban	0.06	1.85	9	2
Bio farm	rural	-	-	2	0

Table 4 gives an overview of the mean and maximum UHI intensities for the urban and urban park locations. Note that the UHI effect is very small at all locations during the day and much higher at night.

The central urban location (Lyceum) exceeded the 18°C and 20°C nocturnal thresholds on 13 and 6 days respectively, the Stadspark station recorded 9 and 2 days respectively, and the rural location exceeded the temperatures on 2 and 0 days respectively.

4.2.1.2 Mobile measurements

In addition to the fixed in-situ measurements, measurements were conducted using a mobile platform, consisting of a car equipped with a number of sensors, including actively and passively ventilated temperature sensors, as shown in Figure 22.

Figure 22 – Actively and passively ventilated temperature sensors, mounted on the car used as a mobile platform. The actively ventilated shield is powered by the car battery's 12 V connection. In the analysis below, we only use data from the actively ventilated measurements.

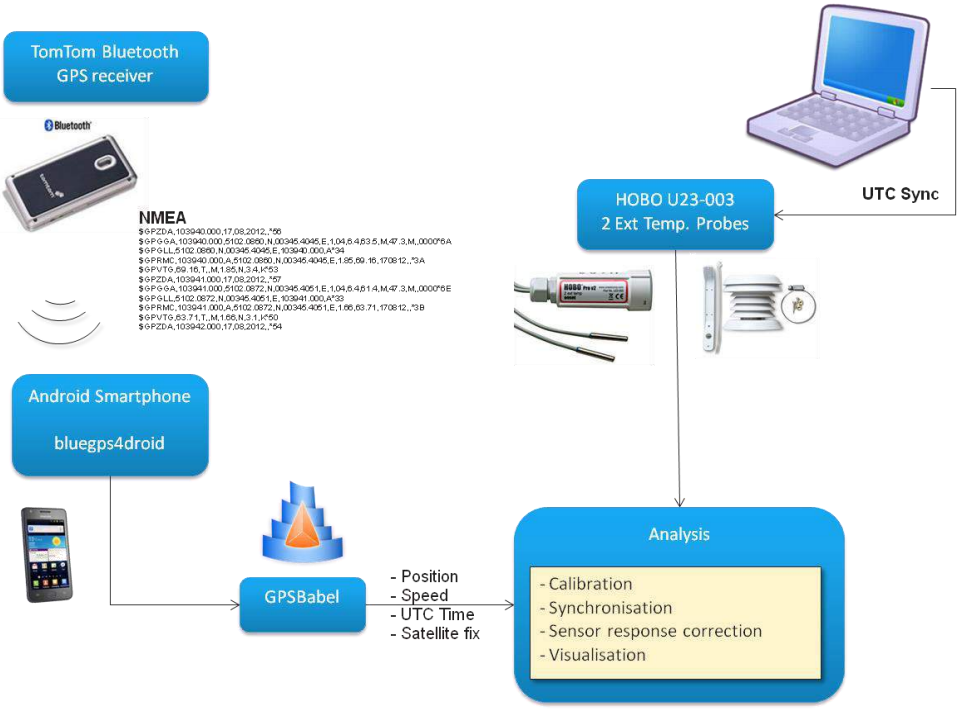

Figure 23 – Scheme of the data-processing system.

The measurements were acquired during the afternoon and evening of 4 September 2013, a late summer day with daytime maximum temperature values near 29°C.

An actively ventilated sensor shield was preferred, in spite of the high "natural" ventilation rate normally experienced by a sensor on a moving car, for the reason that at times the car is forced to stop (e.g. at traffic lights), which could thus adversely affect the accuracy of the measurement at those particular times. Temperatures from the HOBO temperature sensors were synchronized with data from the GPS receiver so as to obtain an accurate positioning of each measurement. The processing chain of all the data is graphically depicted in Figure 23.

As the daytime measurements revealed little or no spatial variation in the air temperature, further focus was on night-time values. However, in contrast to expectations, it turned out that the passively ventilated measurements were the preferred ones. Indeed, it turned out that the natural ventilation caused by the car was more than adequate most of the time. The potential drawback of reduced ventilation when the car had to stop was compensated for by the fact that the passively ventilated system appeared to have a much reduced response time, which enabled much better spatial accuracy. Therefore, only the passively ventilated measurements are used in the further analysis.

The cooling rate was also compensated in order to give the duration of the trajectory of typically one hour, combined with the fact that during this time period an overall cooling rate of the order of 1°C was estimated. It is important to correct for this, as otherwise the final stretches of the trajectory would appear to be miraculously cooler for the wrong reason (i.e. not related to any landscape feature). Consequently, the background cooling rate was corrected for by adding a temperature increment proportional to the elapsed time.

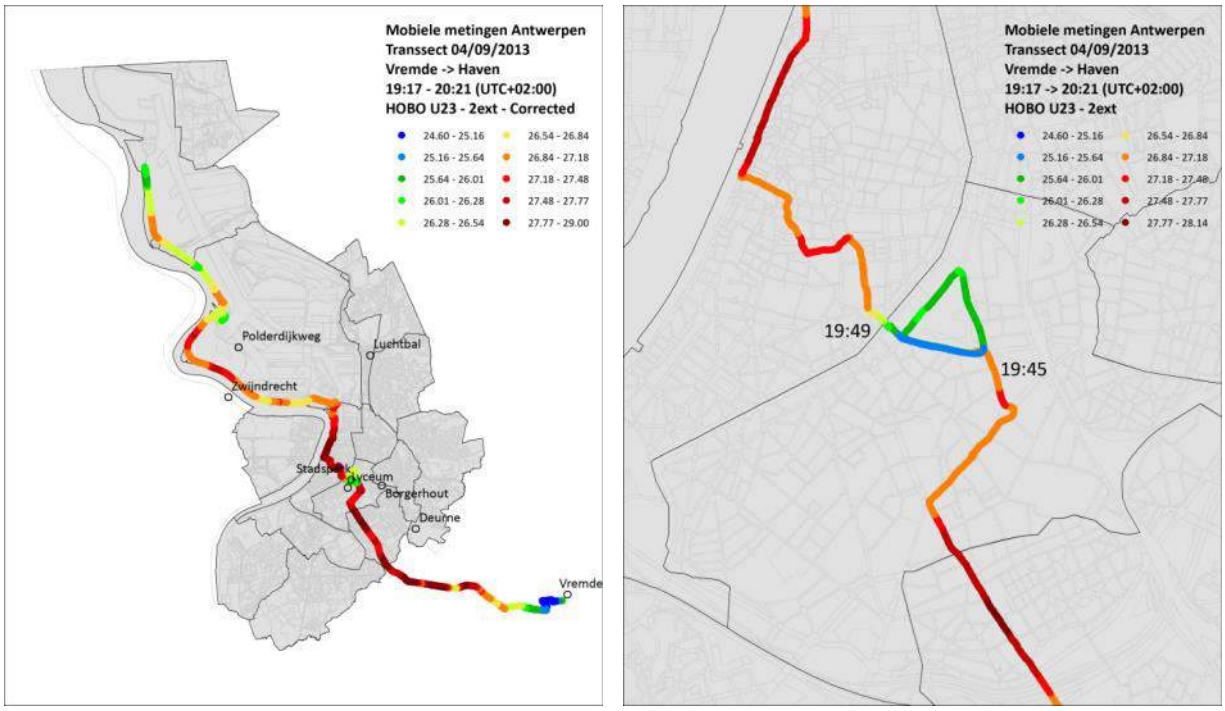

Figure 24 – Temperature over the trajectory run on 4 September 2013. The right panel is zoomed in on the Stadspark (triangular area in the middle).

The car was driven along a trajectory starting at the bio farm (rural) station at 19:17, crossing the entire city up to the harbour area (arrival there at 20:21), passing near the Stadspark in the process. The temperature variation over this trajectory is shown in Figure 24, clearly displaying the urban–rural temperature gradient. More importantly for this report, the cooling effect of the Stadspark stands out very clearly, with temperatures 1–2°C lower than those in the nearby densely built urban zones.

4.2.1.3 Microscale modelling

Microscale simulation experiments were conducted on Groenplaats city square. This large square, located in the centre of the city of Antwerp, is currently in a re-design project phase, and the municipality of Antwerp is currently investigating alternative spatial designs involving additional green infrastructure. The simulations, commissioned

by the city of Antwerp, were conducted in order to assess the benefits of the trees on local thermal comfort experienced on the square and its surroundings.

Figure 25 – The Groenplaats (green square) in Antwerp, the cathedral looming in the background.

The microscale urban climate model ENVI-met model (version ENVI-met 3.0) was used [52], which enables calculation of the fine-scale 3D fields of wind, temperature, radiation and humidity.

To configure the model domain, several GIS-type digital maps (made available by the city of Antwerp) were used. The large-scale base map contains the contours and height information of the buildings in the city, and an aerial photography-based digital map provides detailed information regarding the position of individual green elements (trees) in the city. Both data elements were merged in a model domain configuration map, as shown in Figure 26. The model had to be configured for the wider area enclosing the Groenplaats, while at the same time yielding sufficient spatial detail for the Groenplaats itself. This resulted in the domain containing 200 × 200 horizontal grid cells, at a spatial resolution of 2 m, yielding a domain of 400 m × 400 m. With respect to vertical resolution in the domain, the presence of Antwerp's 120-m high cathedral constituted a major constraint, requiring a relatively high model top of 300 m.

Fortunately, ENVI-met enables the use of a telescopic grid (i.e. it can deal with a variable vertical grid size), and therefore we defined a vertical discretization with a fine resolution (1 m) near the ground, the resolution decreasing with height. As a result, the required large vertical extent of the model domain could be set up with a limited number of grid nodes (vertical model levels). The ENVI-met model can accommodate different types of material to compose the ground surface. This study used the "pavement" (concrete tiles) type, which abounds in this portion of the city. As regards vegetation, most of it consisted of trees between 6 and 10 m in height. In ENVI-met, this is represented by tree type "T1", which is a deciduous tree 10 m high, with the base of the crown 2 m above the ground. Finally, as no details were available regarding the building materials in the domain, the default building parameters available in ENVI-met were used. Heat stress was calculated for a particular day, 24 July 2012, which was characterized by 2-m air temperatures of approximately 28°C at 13:00 local time, a relative humidity of 30%, and a

light breeze (2 m s^{-1}) from the south-east. This was certainly not an extremely hot day; indeed, analysis of available climate data for Antwerp revealed the temperature to be close to the 95th percentile value, meaning that on average, a summer would have five days warmer than 28°C. Therefore, this day can be taken as a representative warm summer day for Antwerp. Heat stress was quantified through the PMV.

Results of the *ENVI-met* simulation expressed in terms of the PMV are shown in Figure 27. When considering the maximum PMV occurring throughout the day, the entire simulation domain exhibits values in excess of 2, except in some small courtyards that are shaded. Large portions of the domain exhibit values of 4, which represents "extremely uncomfortable" conditions. The trees on the Groenplaats are seen to locally reduce the PMV to values between 2 and 3, largely thanks to the shadow they cast.

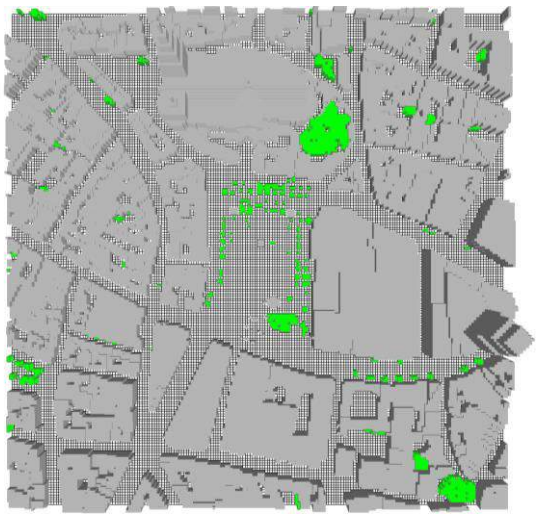

Figure 26 – The model domain used for the Groenplaats assessment. The Groenplaats itself is the large rectangular area in the middle of the domain. The grey shapes correspond to buildings, and trees are indicated in green.

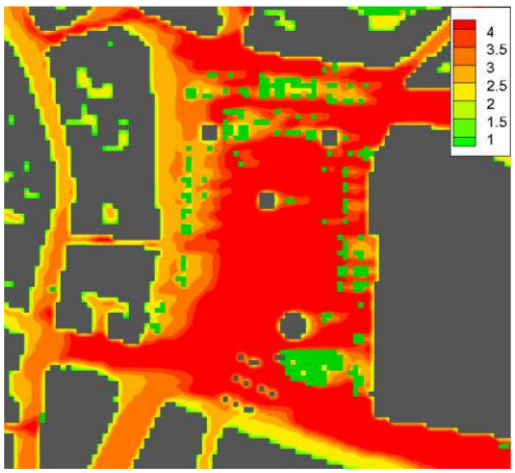

Figure 27 – Average (left) and maximum (right) PMV values on 24 July 2012. Notice the different ranges used in the colour scale.

4.2.2 Bilbao

The study on the city of Bilbao was conducted by NTNU and TECNALIA in collaboration with the municipality of Bilbao.

The municipality of Bilbao is revising the General Masterplan for the city, introducing recommendations by using green infrastructure to mitigate the risk of heat waves in hotspot areas of the city.

The work consists of two parts:

- comparative analysis of green actions to improve outdoor thermal comfort inside typical urban street canyons of three urban areas of Bilbao mostly affected by the risk of heat wave [110]; and
- generalization of the first part of the work analysing the effects of orientation, aspect ratio, ground surface material and vegetation elements on thermal stress inside typical urban canyons.

The following sections present the most relevant outcomes of the study.

4.2.2.1 Green actions to improve thermal comfort in typical urban canyons

The first part of the study conducted in Bilbao consists of a comparative analysis of green actions to improve thermal comfort at pedestrian level in typical urban canyons by studying different greening scenarios.

The simulated scenarios include the current situation (S0), the reconversion in pedestrian streets (S1), testing different green infrastructure, such as grass (S2), grass and trees (S3), green roofs (S4), and combinations of these (S5 and S6) (Figure 28).

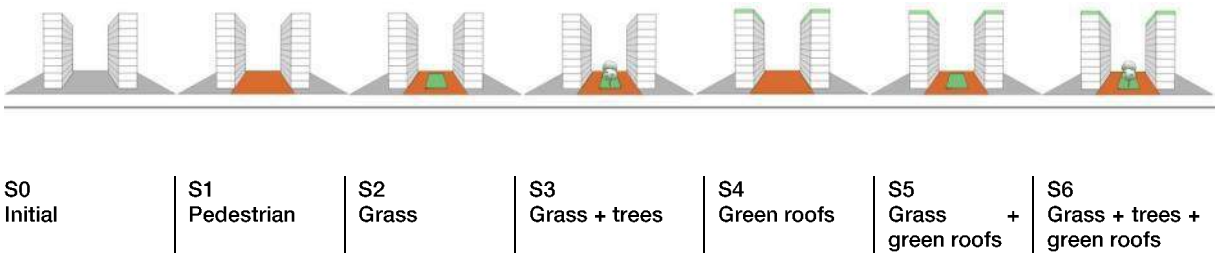

Figure 28 – The scenarios of greening mitigation actions analysed in the city of Bilbao.

The evaluation was performed in three urban street canyons characterized by different aspect ratios: a height/width (H/W) ratio of 1.3 “compact low-rise” exemplified by *Casco Viejo*, H/W ratio of 1.5 “compact mid-rise” exemplified by *Abando/Indautxu*, and H/W ratio of 3.5 “open-set high-rise” exemplified by *Txurdinaga*.

These urban areas were the hottest in the city of Bilbao [61]. Their urban features are as follows:

- *Compact low-rise* (i.e. *Casco Viejo*): buildings are generally residential and commercial blocks of four to six stories and mostly attached one to the other. The area is typical of the historical area of the city, characterized by high density and narrow streets. No green areas are present.
- *Compact mid-rise* (i.e. *Abando/Indautxu*): buildings are generally seven to ten stories high. It is a typical residential and commercial high-density area in the city centre with attached buildings. Streets are mostly narrow with one traffic lane and parking lanes, but wider avenues of four traffic lanes are also present. Green areas are scarcely present.
- *Open-set high-rise* (i.e. *Txurdinaga/Miribilla*): buildings are generally high-rise housing blocks with more than nine stories. Open spaces and green areas are common around the buildings.

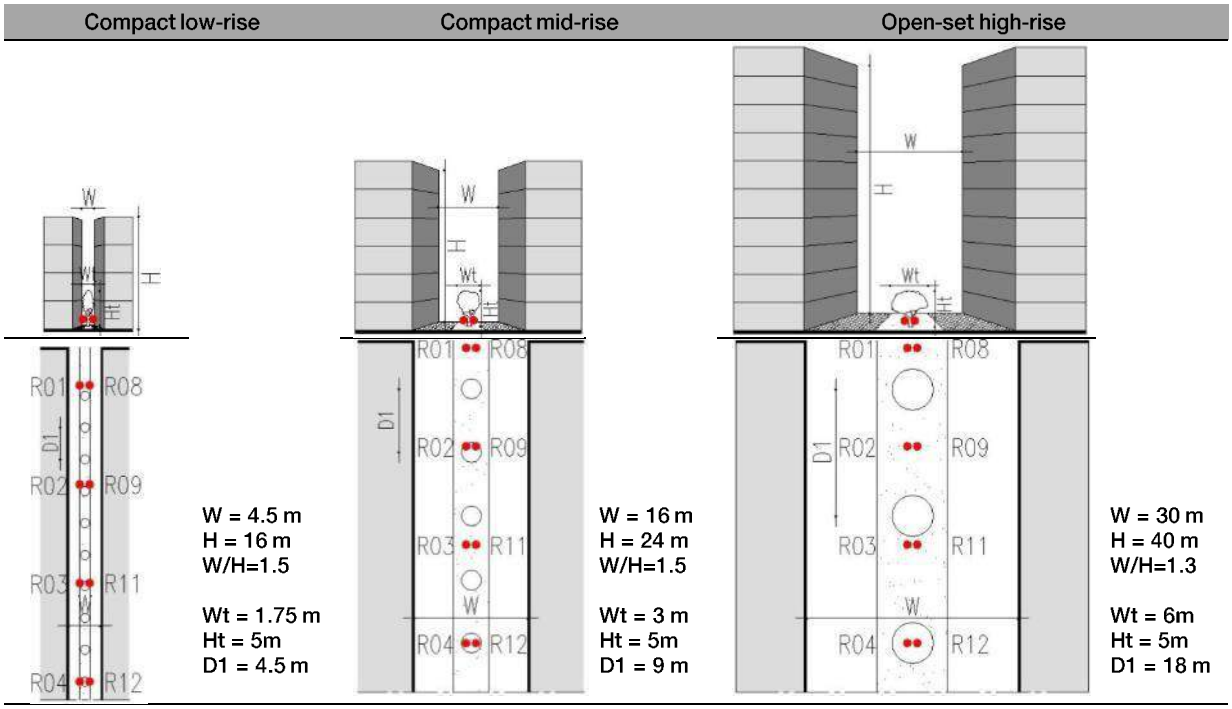

Figure 29 – The analysed urban canyons with the position of the receptors (red dots), trees' location, distance between the trees (D1) and foliage coverage of the trees always maintained equal to 30%. Receptors are selected points inside the model area, where processes in the atmosphere and the soil are monitored in detail. Each receptor contains the complete simulation data (T_{mr}, T_s, T_a, relative humidity, etc.).

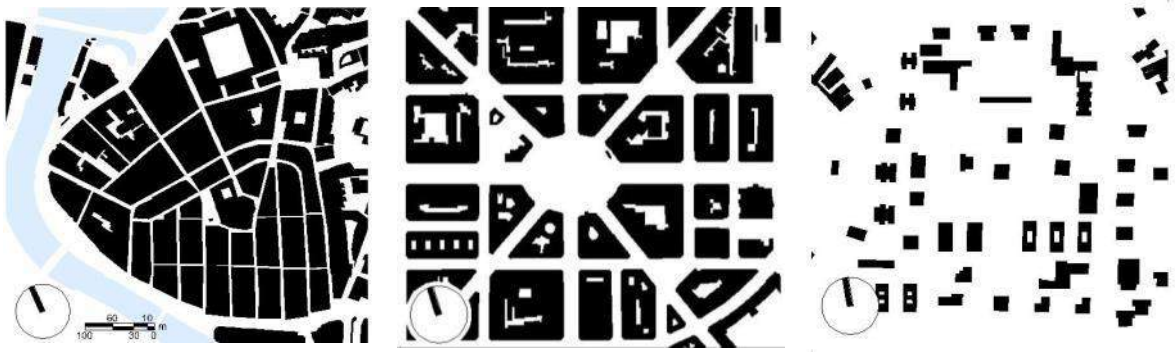

Figure 30 – (From the left) Analysis of the empty and built spaces of the selected urban areas: *Casco Viejo* (high urban building density), *Abando/Indautxu* (medium urban building density) and *Txurdinaga* (low urban building density).

Twenty different scenarios have been evaluated. Using ENVI-met (version ENVI-met 4.0), the spatial and temporal distribution of the meteorological parameters in the selected urban canyons of Bilbao have been simulated. A Fortran matrix was used to calculate the thermal indices of mean radiant temperature, relative humidity, wind speed and PET.

The central part of the ground surface of the street was covered by 30% of grass in order to reproduce the concept of the *Rambla*: a tree-lined pedestrian promenade typical of Spanish cities.

In the compact mid-rise and open-set high-rise urban areas, the decorative red brick stones today replace the asphalt: the streets are converted into pedestrian promenades and they are totally or partially closed to ordinary traffic with use limited to local residents and service and emergency vehicles.

Therefore, both soil asphalt and decorative red brick stone have been tested in compact mid-rise and open-set high-rise urban areas.

The vegetation elements were designed as follows: (i) 50 cm of grass in the central part of the street covering 30% of the total surface of the width of the street, (ii) green roof with 50 cm of grass, and (iii) trees with a height (H_t) of 5 m in all urban areas, while the width of the crown (W_t) was modelled in line with the street width (W). It was set to 1.5 m in the compact low-rise building, 3 m in the compact mid-rise building and 6 m in the open-set high-rise building. The distance between the aligned trees (D1) was set equal to 4.5 m in the compact low-rise building, 9 m in the compact mid-rise building and 18 m in the open-set high-rise building (Figure 29). These settings allowed us to maintain a constant ratio of foliage coverage ($D1/W_t$) equal to 33% in all urban areas

In the typical selected districts, the urban street canyons are mainly oriented as follows: 24^0 north-north-east in *Casco Viejo*; 17^0 north-north-east in *Abando/Indautxu*; and 9^0 north-north-east in *Txurdinaga/Miribilla* (Figure 30). Therefore, the orientations of the models have been set according to the specific prevalent orientation of the urban canyons of the districts. The height of the building and the width of the street were fixed according to the aspect ratio of the urban street canyons.

The analysed scenarios were run on 6th and 7th August in order to simulate the typical summer day conditions in Bilbao. The hourly meteorological data on 7th August 2010 was considered as a representative day of the regional meteorological conditions that affect Bilbao urban areas in summer [111]. The weather data used as input in order to represent the evolution throughout the day was provided by the meteorological station of *Deusto* located in the northern part of the city at 3 m above sea level (latitude 43.28N, longitude 2.93W) [112].

The study quantitatively confirms that vegetation elements such as grass, green roofs and trees improve the thermal comfort at pedestrian level.

Thermal comfort is assessed using the PET thermal index.

Scenario S2 – Effect of grass

In scenario S2, 50 cm of grass in the central part of the street covering 30% of the total surface of the width of the street has been set for all the analysed urban areas.

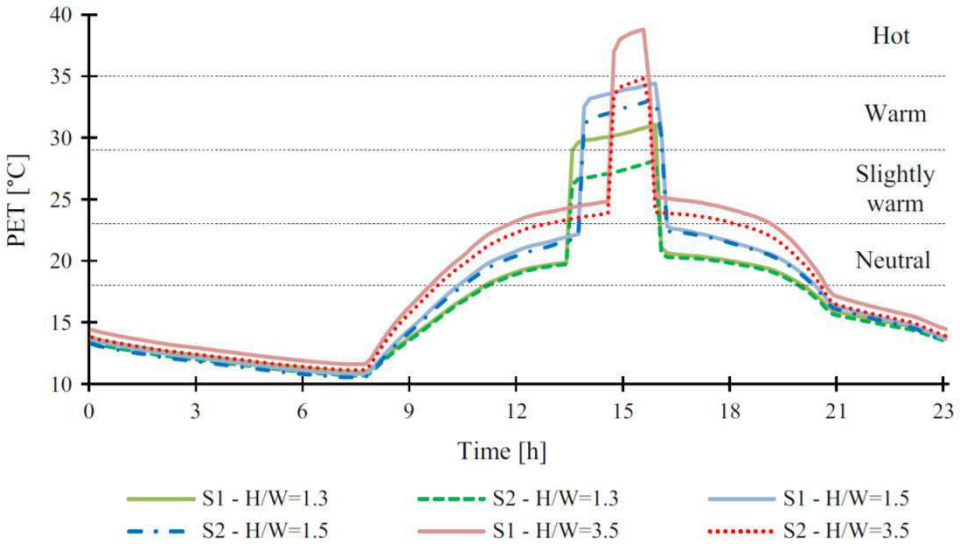

Figure 31 – The profiles of PET for scenarios S1 and S2 within the central part of the Urban Canopy Layer (UCL) at 1 m height considering the different aspect ratios: H/W=3.5 compact low-rise, H/W=1.5 compact mid-rise and H/W=1.3 open-set high-rise.

The presence of grass in the central part of the urban canyon gives benefits in terms of reducing the surface temperature and the mean radiant temperature; it also contributes to reducing the PET level.

The benefits in terms of heat stress reduction are lower in all urban areas since the PET level is lower than in the pedestrian scenario (S1): the presence of grass leads to a reduction of heat stress from the moderate (29°C < PET < 35°C) to the slightly warm level (23°C < PET < 29°C), with a reduction of 3.17 ^{0}C in relation to S1. However, from the analyses, it is clear that the presence of grass has a benefit for all urban canyons (Figure 31).

The highest PET reduction occurs by combining the presence of trees and grass, which can lead to a reduction of about two PET thermophysiological assessment classes during the daily maximum values.

Scenario S3/S6 – Effect of the grass and trees

The cooling effect of the trees was calculated comparing scenario S3 (presence of trees in the urban canyon) with scenario S1 (no trees).

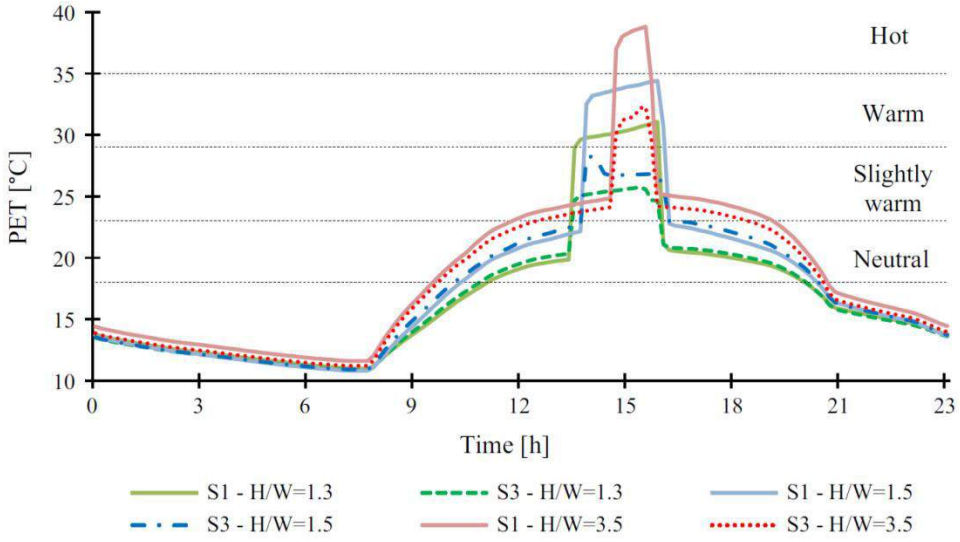

Figure 32 – The profiles of PET in scenarios S1 and S3 within the central part of the UCL at 1 m height considering the different aspect ratios: H/W=3.5 compact low-rise, H/W=1.5 compact mid-rise and H/W=1.3 open-set high-rise.

According to the simulations, the presence of the trees gives a local benefit to the area covered by their shadow due to their geometry (height, shape and width of the crown) and the density of the crown. The highest thermal benefit happened in the central part of the urban canyon (Figure 32), where the lowest thermal benefit in terms of PET level has been registered. By comparing this with the initial scenario (S0), the highest reduction of PET level is equal to 4^{0}C in all urban areas. The same benefits were noticed in scenario S6 where the presence of trees and grass is combined with the presence of green roofs.

Scenario S4/S5/S6 – Effect of the green roofs

The analyses demonstrate that the thermal benefit of green roofs on high temperatures at the pedestrian level is very low. The reduction is nearly absent in the compact low-rise case, while in the compact mid-rise and open-set high-rise urban areas, there is a maximum reduction of PET of around 1^{0}C.

Table 5 summarizes the results of all simulations and scenarios.

Table 5 – Average values of the peak values of PET, Wind Speed (WS), Mean Radiant Temperature (T_{mr}), Relative Humidity (Hr) and Surface Temperature (T_s). Data extracted along the urban canyon in all scenarios.

Scenario		PET [^{0}C]	T_{mr} [^{0}C]	T_s [^{0}C]	T_a [^{0}C]	Hr [%]	WS [m/s]
Compact low-rise	S1	39.23	66.67	34.35	23.22	72.6	1.42
	S2	35.01	58.09	24.35	23.16	72.8	1.38
	S3	32.53	51.70	22.95	23.21	73.2	1.33
	S4	39.10	66.95	34.05	23.30	73.1	1.32
	S5	35.00	58.00	24.45	23.25	73.3	1.31
	S6	32.29	51.64	23.05	23.25	73.6	1.24
Compact mid-rise	S0	32.99	60.98	34.25	24.21	72.5	3.10
	S1	34.72	65.67	31.75	23.97	72.5	3.10
	S2	31.76	61.10	26.45	23.73	73.5	2.76
	S3	28.73	57.83	22.85	23.59	73.7	2.15
	S4	33.68	65.46	31.05	23.78	72.0	3.48
	S5	31.51	61.33	26.65	23.68	72.9	3.11
	S6	28.08	50.55	23.95	23.42	73.0	2.45
Open-set high-rise	S0	29.91	61.53	36.85	22.95	67.6	4.23
	S1	31.53	65.94	33.75	22.88	67.6	4.23
	S2	28.37	55.91	24.95	22.91	68.6	3.79
	S3	26.79	50.37	23.65	23.02	69.4	3.20
	S4	30.30	65.76	33.15	22.61	65.9	4.41
	S5	27.34	56.15	24.95	22.58	66.3	4.16
	S6	25.85	45.29	22.45	22.75	68.1	3.07

4.2.2.2 Effect of the street's finishing materials

The reconversion of an ordinary vehicle traffic road into pedestrian boulevards has become a typical transformation intervention in compact mid-rise and open-set high-rise urban areas of Bilbao during the last decade. The asphalt ground is usually replaced with decorative red brick stones and the streets are totally or partially closed to motor traffic in order to create dedicated pedestrian fluxes and public urban spaces (Figure 33). Service and emergency traffic and resident access are still allowed. In contrast, in the compact low-rise urban area, such as the historic centre, the traffic was limited to local residents, and service and emergency vehicles a long time ago. The ground surface of the street is entirely covered by decorative red brick stone (S1). Therefore, scenario S0 for compact low-rise urban areas has not been considered.

Lutxana Kalea | Ercilla Kalea | Indautxu Kalea | Santiago de Compostela Kalea

Figure 33 – (From the left) Visualization of pedestrian boulevards in the area of *Abando/Indautxu* (compact mid-rise, e.g. *Lutxana Kalea, Ercilla Kalea*) and *Miribilla* (open-set high-rise, e.g. *Indautxu Kalea* and *Santiago de Compostela Kalea*).

The conducted analyses in the compact mid-rise and open-set high-rise urban areas gave significant results in terms of reduction of PET level. In both urban areas, the two different ground materials asphalt and red brick stones, have been tested. The data shows how the ground materials' different albedo (0.12 for asphalt and 0.30 for red brick stone) affects the surface temperature (T_s,) the mean radiant temperature (T_{mrt}) and consequently the PET. During the peak period, the T_s increases by more than 10^0C, while the T_{mr} increases by more than 3^0C.

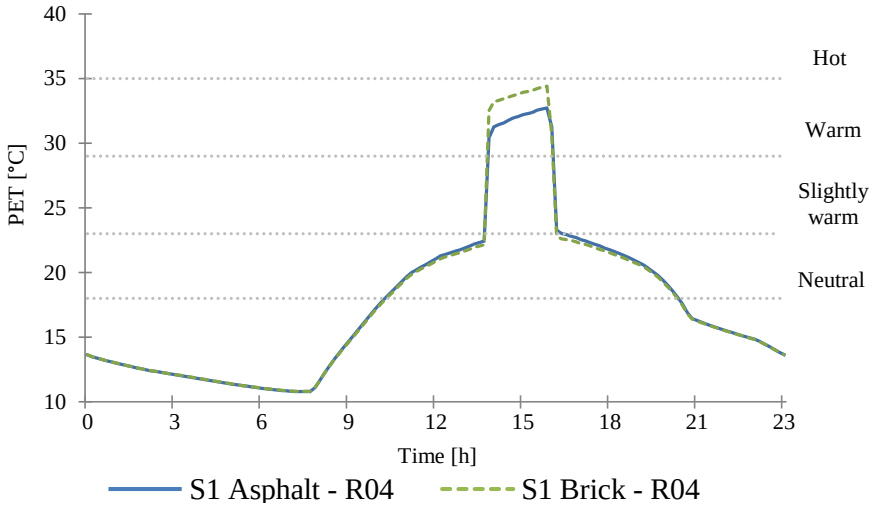

Figure 34 – Typical PET trend – compact mid-rise.

This phenomenon is strictly linked to the ratio aspect (H/W) of the urban canyon and to the orientation of the district.

The T_s results are higher in the pedestrian scenario with decorative red brick stones than when using asphalt. The biggest difference between the two finishing materials is equal to 2.52^0C at 15:40 in the compact mid-rise urban areas, while in the open-set high-rise the difference reaches 3.13^0C at 15:50. Furthermore, the results for the T_s for the two finishing materials are higher in the open-set high-rise than in the compact mid-rise district. This is due to the longer duration of the peak period: the ground remains exposed for half an hour more in the open-set high-rise given the geometry of the UCL. Furthermore, the trends of the T_s demonstrate that the temperature of the ground in asphalt increases and decreases more quickly during the daytime and night-time. Regarding the T_{mr}, the red brick stone scenarios come out with higher values than the scenarios with asphalt. This is due to a combination of two reasons: on the one hand, wind speed is influenced by the aspect ratio of the urban canyon but on the other hand, urban geometry conditions are affected by solar radiation inside the UCL. Thus, heat accumulation (i.e. T_{mr} and T_s) is influenced not only by solar radiation but also by wind speed. The T_s and the T_{mr} consequently affect the values of thermal comfort: during the peak period, the difference between the two materials is more than 1.5^0C in both urban areas (1.73^0C in the compact mid-rise and 1.63^0C in open-set high-rise). Despite all the values being within the moderate warm level of heat stress, the differences between the two urban areas are quite significant. Therefore, the PET results are higher in the compact mid-rise than in the open-set high-rise.

4.2.2.3 Effects of orientation, aspect ratio, ground materials and vegetation on thermal stress inside typical urban canyons

The second part of the study tested the benefits of the green elements using a parametric analysis in the urban canyons that have been analysed in the first part. Specifically, the purpose of this part of the work was to generalize the outcomes in order

to provide recommendations for urban greening strategies, not only for consolidated urban areas but also for development of new districts. The analyses were conducted using *ENVI-met* on typical summer day conditions (7th August), considering the four standard orientations (i.e. E–W, N–S, NE–SW and NW–SE) and the various aspect ratios (H/W). The PET index in 40 different scenarios has been evaluated. The benefits of planting grass and trees in urban canyons were studied according to the following scenarios:

(i) Mitigation 01: the height of the trees was set equal to 5 m and the height of the grass equal to 10 cm (Table 6);

(ii) Mitigation 02: the height of the trees was proportionally set to the height of the analysed urban canyons. Therefore, the ratio H_{tree}/H_{canyon} = 0.25 was maintained constant (Table 7); and

(iii) Mitigation 03: the height of the trees was maintained as in the previous scenario, while the width of the tree was proportionally set to the width of the analysed urban canyons. Therefore, both ratios H_{tree}/H_{canyon} = 0.25 and W_{tree}/W_{canyon} = 0.3 were maintained constant (Table 8).

All these settings were tested for each standard orientation.

Table 6 – Settings for mitigation 01

Mitigation 01 – Trees of the same height – 5m						
Urban area	Urban canyon (height/width)	Ground material	Grass	Trees	H_{tree}/H_{canyon}	W_{tree}/W_{canyon}
Compact low-rise	16 m /4.5 m (3.5)	Brick	10 cm	B5 – Tree 5 m; crown full of leaves	0.31	0.44
Compact mid-rise	24 m /16 m (1.5)	Brick/Asphalt	10 cm	P1 – Platanus 5m; crown full of leaves	0.20	0.12
Open-set high-rise	40 m /33 m (1.3)	Brick/Asphalt	10 cm	P1 – Platanus 5m; crown full of leaves	0.12	0.06

Table 7 – Settings for mitigation 02

Mitigation 02 – The height of the trees were set in order to maintain a constant ratio: H_{tree}/H_{canyon}= 0.25						
Urban area	Urban canyon (height/width)	Soil	Grass	Trees	H_{tree}/H_{canyon}	W_{tree}/W_{canyon}
Compact low-rise	16 m /4.5 m (3.5)	Brick	10 cm	A1 – Tree 4 m; 1/2 without leaves	0.25	0.3
Compact mid-rise	24 m /16 m (1.5)	Brick/Asphalt	10 cm	A2 – Tree 6 m; 1/2 without leaves	0.25	0.12
Open-set high-rise	40 m /33 m (1.3)	Brick/Asphalt	10 cm	A3 – Tree 10 m; 1/2 without leaves	0.25	0.06

Table 8 – Settings for mitigation 03

Mitigation 03 – The height and the width of the trees were set in order to maintain constant ratios: H_{tree}/H_{canyon}= 0.25 W_{tree}/W_{canyon}= 0.3						
Urban area	Urban canyon (height/width)	Soil	Grass	Trees	H_{tree}/H_{canyon}	Wt_{ree}/W_{canyon}
Compact low-rise	16 m /4.5 m (3.5)	Brick	10 cm	A1 – Tree 4 m; 1/2 without leaves	0.25	0.3
Compact mid-rise	24 m /16 m (1.5)	Brick/Asphalt	10 cm	P6 – Platanus 6m height and 5m width; 1/2 without leaves	0.25	0.3
Open-set high-rise	40 m /33 m (1.3)	Brick/Asphalt	10 cm	P2 – Platanus 10 m height and 11 m width; 1/2 without leaves	0.25	0.3

4.2.2.4 Impact of urban density, geometry, orientation and aspect ratio of UCL

First, the current initial situation was analysed (S0) and then the effect on thermal stress by replacing asphalt with decorative red brick stones for the ground finishing material was calculated (S1).

The most important aspect that consistently affects the peak of PET, its duration and the period of thermal discomfort (PET > 23°C) at the pedestrian level is the orientation.

The results of the worst orientation (45^0 NE–SW) demonstrate that the highest level of thermal stress (PET > 41^{0}C) has been reached in all urban districts, even if the intensity of the peaks is extremely different from one area to another (Table 9). Another relevant aspect that has to be observed is the shifting and the duration of the peaks' intensity as well as the duration of the thermal discomfort (PET > 23°C) within the UCL, which varies consistently in each urban area due to the orientation of the district.

Table 9 – Values of peaks, duration of the intensity of peaks and duration of thermal discomfort (PET > 23 ^{0}C) within the analysed urban areas at the pedestrian level (data corresponds to the location with the highest PET value).

Level of heat stress – PET Current initial situation (S0)		Compact low-rise H/W = 3.5; Ground in brick		Compact mid-rise H/W = 1.5; Ground in asphalt		Open-set high-rise H/W = 1.3; Ground in asphalt	
		24^0 NE–SW	45^0 NE–SW	17^0 NE–SW	45^0 NE–SW	9^0 NE–SW	45^0 NE–SW
Intensity of peaks	^{0}C	39.23	51.56	32.99	46.84	29.91	45.67
Duration of the intensity of peaks	Time	1 hour (from 14:40 to 15:40)	1 hour (from 15:30 to 16:30)	2 hours (from 13:40 to 15:40)	2 hours and 20 minutes (from 14:40 to 17:00)	2 hours and 20 minutes (from 13:30 to 15:50)	2 hours and 40 minutes (from 14:30 to 17:10)
Duration of thermal discomfort (PET > 23 ^{0}C)	Time	7 hours and 20 minutes (from 11:40 to 19:00)	11 hours (from 09:20 to 20:20)	6 hours and 10 minutes (from 12:00 to 18:10)	10 hours and 30 minutes (from 09:50 to 20:20)	2 hours and 20 minutes (from 13:30 to 15:50)	10 hours (from 10:10 to 20:10)

The difference between compact low-rise and open-set high-rise urban areas is quite consistent, given that the PET goes from strong (35^{0}C < PET < 41^{0}C) to moderate heat stress (29^{0}C < PET < 35^{0}C). The peak values coincide with the presence of direct solar radiation.

The duration of the peak's intensity is different in each urban canyon due to the orientation and the aspect ratio (H/W). The both factors contribute on the intensity of thermal stress and shift the peak period and the influence of solar radiation within the UCL. In this specific case, by analysing the intensity of the heat stress and the duration of the peak period, it is notable that the highest value of PET level is reached in the compact low-rise urban areas.

The comparison of the worst situation (45^0 NE–SW) with the actual situation using the most prevalent orientation of the street of the three selected urban areas studied in the first part showed that the PET increase peaks consistently as well as the duration of thermal discomfort during the day (Table 9).

For example, during a one-hour peak in the compact low-rise, from 2:40 pm to 3:40 pm, the temperature is around 40^{0}C, within the range of strong heat stress (35°C < PET < 41°C) at the pedestrian level. This is caused by the aspect ratio of the UCL and the presence of low wind speed (average values 1.3 m/s). In the compact mid-rise and open-set high-rise, the maximum level of heat stress is moderate.

However, the peak values between the two urban areas has a difference of more than 3°C and the duration of the highest intensity of PET is shifted by half an hour.

While in the compact mid-rise the duration of the peak is from 1:40 pm to 3:40 pm, in the open-set high-rise it varies from 1:30 pm to 4:00 pm. This is mainly caused by the influence of solar radiation that remains over 750 W/m^2 for the entire peak period.

The registered wind speeds in both urban areas are higher than in the compact low-rise urban areas: the average values are equal to 2.74 m/s in the compact mid-rise and 3.74 m/s in the open-set high-rise. In the compact mid-rise and open-set high-rise urban areas, the PET level remains over the limit of neutral heat stress only during the peak period, while due to the aspect ratio and the orientation, in the compact low-rise the duration of thermal discomfort within the UCL at pedestrian level persists for more than 7 hours (from 11:50 am to 7:00 pm), while in the worst scenario (45^0 NE–SW) it lasts for 11 hours.

Regarding scenario S1, as has been demonstrated in the first part of the study, using the decorative red brick stones increases the PET value by more than 2°C in both compact mid-rise and open-set high-rise urban areas (Table 10). However, the duration of peak intensity and the period of thermal discomfort (PET > 23°C) remain the same in comparison with the initial scenarios (S0) in all urban areas.

Table 10 – Average values of maximum PET level, calculated considering all 14 receptors in the UCL for different aspect ratios (H/W = 3.5 in compact low-rise, H/W = 1.5 in compact mid-rise and H/W = 1.3 in open-set high-rise) and orientation. All scenarios with ground in brick have been considered (data corresponds to the location with the highest PET).

S1 pedestrian scenario Reconversion in pedestrian street with ground in brick	Compact low-rise H/W = 3.5		Compact mid-rise H/W = 1.5		Open-set high-rise H/W = 1.3	
	24^0 NE–SW	45^0 NE–SW	17^0 NE–SW	45^0 NE–SW	9^0 NE–SW	45^0 NE–SW
Intensity of peak of PET [^{0}C]	39.23	51.56	34.72	49.29	31.53	48.17

4.2.2.5 Cooling effect of combining grass and trees

Analysing the peak values for all the urban areas, the highest thermal stress is present for the NE–SW orientation. For this orientation, the heat stress remains at the extreme level (PET > 41^{0}C). Therefore, the outdoor comfort within the urban canyon at the pedestrian level is uncomfortable during most of the day.

Only in the open-set high-rise urban areas does the PET decreases from extreme heat stress (PET is equal to almost 46^{0}C) stress (PET is equal to almost 46^{0}C) to strong heat stress (PET reaches 40.6^{0}C). The lowest peak values are reached in the lowest peak values are reached in the NW–SE orientation in all urban areas. The level of thermal comfort in the urban thermal comfort in the urban canyon improves for the N–S and W–E orientations. It passes from moderate (initial scenario) passes from moderate (initial scenario) to slightly warm level in compact mid-rise and open-set high-rise urban areas (

open-set high-rise urban areas (

Table 11).

However, for the urban canyon in proximity of the trees, the thermal benefit is higher due to the presence of the vegetation elements.

For example, in the compact low-rise, the results demonstrate that locally at the centre of the urban canyon the PET for the NE–SW orientation passes from the extreme (PET equal to 52.9°C in the initial scenario) to the strong level (PET reaches 40.4°C in mitigation 02/03 scenario) and the reduction is more than 12^{0}C. The lowest peak values are reached in the NW–SE orientation. The heat stress in this specific orientation varies from strong (PET reaches 31.9°C in the initial scenario) to slight (PET is equal to 27.2°C in mitigation 01/02/03). In the compact mid-rise urban areas, at the same point, the PET level passes from the extreme (PET level is 49.4°C in the initial scenario) to strong level (PET reaches 37.3°C in mitigation 03) and the reduction in terms of temperature is more than 12^{0}C. The lowest peak values are reached in the NW–SE orientation. In analysing the daytime period, the level of heat stress decreases from slight (PET is 29°C in the initial scenario) to neutral (PET reaches 26.9°C in mitigation 03) thanks to the mitigation effect created by the presence of grass and trees.

Table 11 – The maximum value of the PET considering all receptors in all different mitigation scenarios.

Peak values of PET in all urban areas for different mitigation effects – all receptors						
				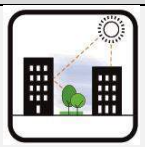		
Urban areas	Orientation		Initial	Mitigation 01 (Trees with same height)	Mitigation 02 (H_{tree}/H_{canyon}= 0.25)	Mitigation 03 (H_{tree}/H_{canyon}= 0.25 W_{tree}/W_{canyon}= 0.3)
 Compact low-rise	Brick	N–S	35.33°C	32.53°C	33.40°C	33.40°C
		NE–SW	52.97°C	45.84°C	47.17°C	47.17°C
		NW–SE	32.94°C	30.92°C	31.59°C	31.59°C
		W–E	33.67°C	30.32°C	30.97°C	30.97°C
 Compact mid-rise	Brick	N–S	33.47°C	32.53°C	33.66°C	32.33°C
		NE–SW	50.90°C	43.21°C	44.83°C	43.49°C
		NW–SE	29.20°C	27.51°C	27.41°C	26.13°C
		W–E	33.18°C	30.34°C	31.70°C	29.87°C
	Asphalt	N–S	31.70°C	30.54°C	31.55°C	30.43°C
		NE–SW	48.03°C	43.32°C	44.94°C	43.61°C
		NW–SE	30.20°C	28.57°C	29.50°C	28.02°C
		W–E	31.57°C	30.44°C	31.03°C	30.32°C
 Open-set high-rise	Brick	N–S	30.84°C	28.89°C	29.27°C	28.32°C
		NE–SW	48.34°C	40.83°C	41.90°C	40.39°C
		NW–SE	27.01°C	25.53°C	26.86°C	25.47°C
		W–E	31.66°C	28.77°C	29.17°C	29.35°C
	Asphalt	N–S	29.19°C	28.98°C	29.21°C	28.50°C
		NE–SW	45.99°C	40.98°C	41.04°C	40.61°C
		NW–SE	26.43°C	25.10°C	26.57°C	25.00°C
		W–E	29.98°C	28.84°C	29.64°C	28.39°C

In the open-set high-rise, the same local effect gives the highest thermal stress for the NE–SW orientation, where the PET level goes from extreme (PET level is 48.2°C in the initial scenario) to strong (PET reaches 32.8°C in mitigation 03) and the reduction in terms of temperature is more than 15°C. Also in this urban area, the lowest peak values are reached in the NW–SE orientation. The thermal stress in this specific orientation varies from moderate (PET level is 25.8°C in the initial scenario) to neutral (PET reaches 22°C in mitigation 03).

The results of the highest peak values of PET within the urban canyons in all urban areas for different mitigation scenarios for different mitigation scenarios are summarized in

Table 11.

The results demonstrate that the level of PET depends on the aspect ratio of the urban canyon. In particular, the PET varies from extreme to slightly warm thermal sensitivity, which corresponds to the highest heat stress in the compact low-rise urban areas to the slight heat stress in the open-set high-rise ones (Figure 35). However, the PET values can reach the neutral level of heat stress locally in some parts of the urban canyons in the NW–SE and W–E orientations in compact mid-rise and open-set high-rise urban areas. The urban density and aspect ratio (H/W) of the urban canyon influence thermal stress at the pedestrian level. For example, in the compact low-rise urban areas, the morphology of the urban canyon, characterized by narrow width of the street, contributes to maintaining the PET level over the threshold of extreme heat stress. In fact, in this urban

area, despite the reduction of PET by more than 7°C in relation to the initial scenario, the highest PET peak has been registered.

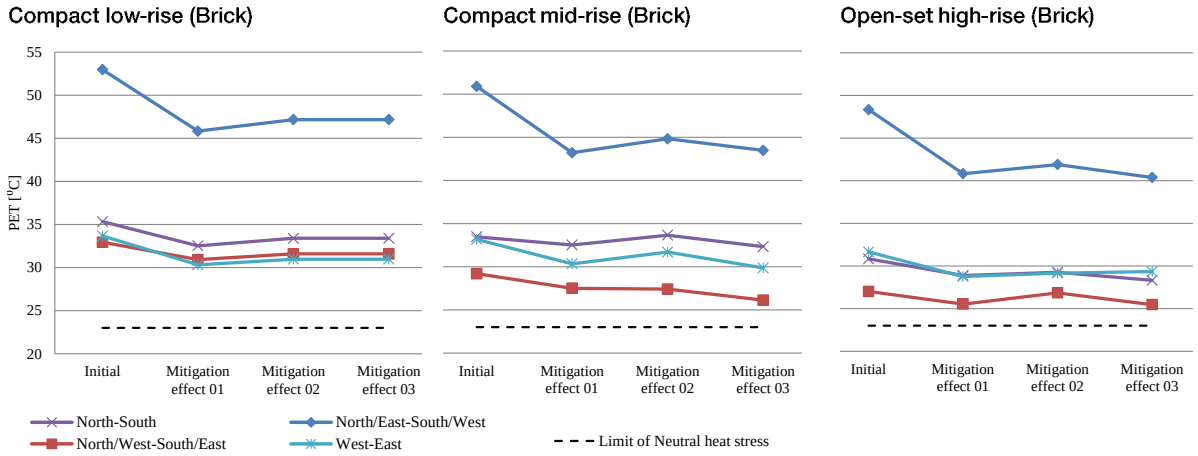

Figure 35 – Trend of the peak values of PET for all the mitigation effects in the different urban areas – all receptors.

One of the most important aspects that came out from the analyses is that the mitigation effect given by the presence of vegetation elements, such as trees, is locally limited and it strongly depends on the shape of the trees and the foliage's crown density. The choice of tree type is one of the most important decisions to make, given their influence on the thermal comfort within the urban canyon. Another important aspect that influences the thermal stress in the urban canyon is the wind speed at the pedestrian level. Figure 36 shows a summary of the peak values of the wind speed in all scenarios for the different urban areas and mitigation strategies. The results demonstrate that the wind speed depends on the aspect ratio of the urban canyons, their orientation and the presence of vegetation. It can vary from 0 m/s in the compact low-rise urban areas, when the orientation is NE–SW with respect to the incoming flow, to around 7 m/s in the open-set high-rise (orientation NW–SE).

In the second part of the study, it is possible to better understand the effect of the wind speed on thermal stress comfort within the urban areas. Figure 36 clearly shows how the presence of trees has a relevant contribution to decreasing the wind speed: the reductions can reach more than 2.00 m/s, as happened in the compact mid-rise and open-set high-rise urban areas (orientation NW–SE), while in the compact low-rise urban areas, the wind speed remains practically constant even with the presence of trees, due to increasing the street roughness parameter.

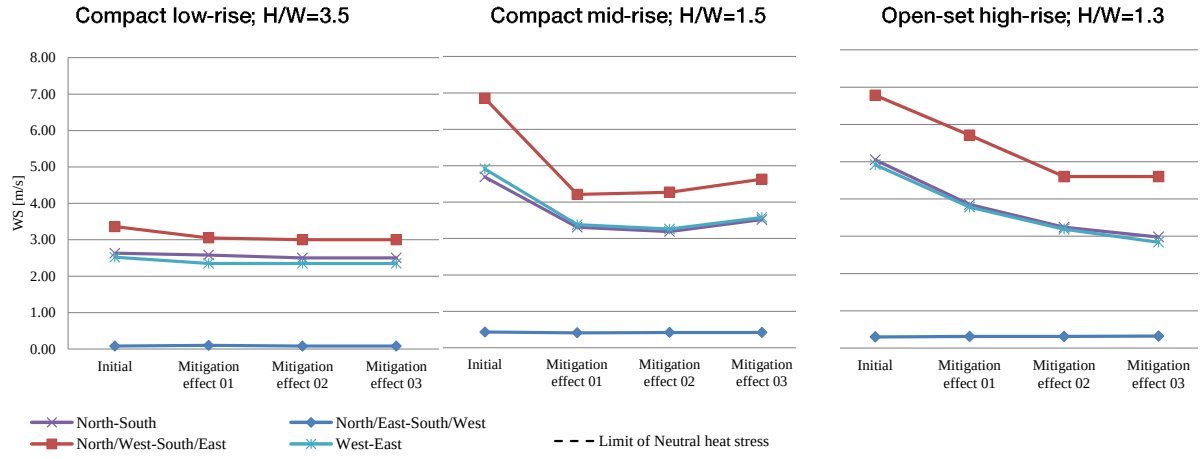

Figure 36 –Wind speed trends in the different urban areas characterized by specific geometry of the urban canyon (ratio height/width of the urban canyon: compact low-rise equal to 3.5, compact mid-rise equal to 1.5 and open-set high-rise equal to 1.2).

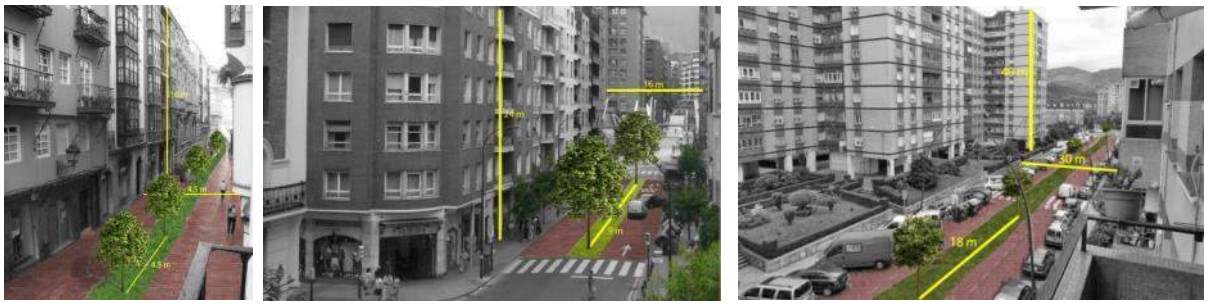

Figure 37 – (From left) Visualization of the green mitigation actions in compact low-rise, compact mid-rise and open-set high-rise urban areas.

5 Discussion

In response to extreme heat events like the one of summer 2003 in Europe, urban planners and city authorities have been attempting to find mitigation scenarios to improve the living conditions for local inhabitants. Usually city planners use green surfaces, highly reflective building materials and a changed building geometry as tools to reduce the effects of heat.

Results from the case study cities can offer decision support to local authorities for a sustainable urban development and contribute to climate research through improved models dealing with urban environments.

5.1 Urban planning recommendations at the mesoscale

Specific urban planning strategies, like green roofs and park areas, have been studied for the cities of Antwerp, Paris and Delhi. This section presents, the most relevant results related to the conducted analyses on the case study cities will be presented.

5.1.1 Antwerp

The analyses show that the heat island effect in Antwerp is present in some hotspot areas in the city, where they are warmer than the rural surroundings as well as the harbour area.

The conducted analyses demonstrated that the effects of green areas are limited to the parts of the city where they are implemented and do not have an impact on the wider environment. The magnitude of this effect is rather limited at the city scale. The conducted analyses on the Stadspark area demonstrated that a high cooling effect is created by the park. However, this effect is strictly limited to the park area and the nearby urban zone.

Therefore, one of the recommendations regarding greening strategies is that the presence of large parks in the city centre brings local cooling. Large parks are definitely preferable to small parks: one big park provides a higher cooling effect than many small ones. This recommendation has to be taken into account when the objective is exclusively the maximization of the cooling effect of the area, even if this effect remains substantially circumstantial around the park itself. However, the presence of smaller parks, where access is easier for people, might be important for local cooling spots during heat wave events. This aspect underlines the importance of having a local presence of vegetation in built-up areas. In fact, locally also where there are small parks,

it reduces the human exposure to high temperature thanks to the shadow area created by the vegetation during the daytime.

The possibility to increase the vegetation cover from around 20–30% to 60% provides a small reduction in terms of heat wave intensity. However, its cooling benefit is more diffuse than the one created by the presence of the park.

Another aspect that could contribute to limiting the nocturnal cooling effect of the city is the roughness length: the higher the roughness of the city, the lower the reduction of UHI intensity.

5.1.2 Paris

The analyses conducted in Paris demonstrated that the UHI intensity of an urban park zone exhibits roughly half the UHI intensity of the surrounding dense urban zones, thus confirming the potential of urban green space as a relevant climate adaptation measure.

Therefore, this study also confirms that the presence of urban parks reduces the UHI intensity, even if the benefit remains strictly localized in the area of the park and its immediately nearby areas.

5.1.3 Delhi

The conducted analyses on urban vegetation abundance in the city of Delhi have shown that an inverse relation exists between areas with sparse vegetation cover which present higher temperatures, and vice versa.

This quantitatively confirms the results obtained in the city of Antwerp in which the presence of larger green areas are preferable given the higher cooling effect in comparison to several distributed green spots.

5.2 Urban planning recommendations at the microscale

The simulation analyses and the on-site measurements conducted at the microscale in the cities of Antwerp and Bilbao have led to some recommendations that will be presented in the next sections.

5.2.1 Antwerp

The results comparing the in-situ measurements conducted in summer 2013 during the diurnal cycle with the data from the bio farm in Vremde confirmed the thermal benefit given by the presence of the Stadspark within the city. The park leads to a reduction in the effect of the UHI during the day, while during the night it remains constantly lower than in the nearby urban areas. However, in all monitored urban areas, from the urban station to the one located in the rural environment, it was quantitatively confirmed that the UHI effect results are lower during the day and higher at night. The strongest average UHI intensity was registered in the urban station.

Another relevant indication of the cooling benefits of the presence of the Stadspark in Antwerp is that it helps reduce the number of UHI events. In fact, the number of nights that exceeded the limit of nocturnal minimum temperature for a heat wave in Belgium were reduced by more than half in the urban areas.

The mobile measurements distinctly show the cooling effect of the Stadspark and how its benefit is extended to the nearby densely built urban areas.

Finally, the analyses conducted in Groenplaats square in the centre of Antwerp showed the importance of planting trees in large urban environments. In fact, the trees reduce the PMV values due to their shadows. However, this benefit remains local to the area in the

shadow of the trees. Therefore, urban furniture such as benches should be placed in suitable positions in order to exploit the benefits of the trees as much as possible.

5.2.2 Bilbao

The intensity of cooling in terms of PET reductions and their spatial extent differed distinctly between the various vegetation measures. Vegetative measures, which were applied inside the street canyons such as tree-lined streets, had a noticeable cooling effect at the pedestrian level.

The case study of Bilbao demonstrated that the tree-lined streets provided a cooling effect within the urban canyon both in terms of PET reduction and local spatial extent. The strongest reductions of 10°C in air temperature were found inside and specifically under the tree crowns.

The effect of the green roofs on PET in the street canyon was also noticeable but relatively small compared to the presence of grass and trees. In the centre of the street canyons, the cooling effect from a green roof was not found in compact low-rise urban areas, whereas it had low influence in the street canyon of compact mid-rise and open-set high-rise (< 1°C). However, for perpendicular or oblique winds, the cooled rooftop air may get entrained into the street canyon and result in noticeable PET reductions. More analyses are necessary in order to study this effect.

The combination of all vegetative measures (trees, grass and green roofs) showed the largest impact on the PET level.

Tree-lined streets are preferable to green roofs because their overall cooling effect is much greater due to their larger vegetation volume and foliage density. In particular, tree-lined streets composed of tree species with tall and broad crowns appear very promising due to the large vegetation volume and leaf biomass inside the canyon. The study clearly showed that the cooling effect was in general locally restricted to within close vicinity of the trees.

From the conducted analyses, it is also evident that urban parameters such as orientation and aspect ratio (H/W) of the urban canyons have a considerable influence on thermal comfort at the pedestrian level. They consistently influence the intensity of the PET level, its duration during the day and the period of thermal discomfort (PET > 23^0C) at the pedestrian level.

It is also important to specify that the results presented in the first part of the study are valid for compact low-rise, compact mid-rise and open-set high-rise urban areas that have the same orientations and the same aspect ratio of the analysed urban canyon of the city of Bilbao. Therefore, the results are strictly related to the analysed districts located in specific parts of the city. In that sense, it is relevant to underline that each city is characterized by specific prevalent wind, and each part of the city has a proper orientation and aspect ratio. However, the methodology for evaluating the cooling effect created by the presence of vegetation, and how the orientation and the aspect ratio could affect the thermal comfort at the pedestrian level of urban canyons could be replicated in different cities.

Another relevant recommendation relates to the thermal effect created by the installation of different finishing materials for the ground. For example, in Bilbao, the increased intervention to convert streets into pedestrian promenades by replacing the asphalt with decorative red brick stones increases the values of T_{mr} and T_s and consequently the PET level at the ground level.

The results also demonstrated that the aspect ratio and the presence of vegetation consistently influence the wind speed values at the pedestrian level and consequently

the thermal benefits in all urban areas. In this sense, has to be underlined that the presence of trees decreases the wind speed in the compact mid-rise and open-set high-rise urban areas, while in the narrow urban canyons as in the compact low-rise urban areas, despite the presence of trees, the wind speed remains practically constant. In those urban areas, the thermal benefit is still very low and localized under the shadow of the threes. While, in the compact mid-rise and open-set high-rise the geometry of the urban canyon characterized by higher width, contributes to maintain a higher cooling effect created by the presence of the wind for the entire extension of the urban canyon.

Both aspect ratio and orientation were found to have a considerable influence on the street thermal comfort in urban environment and consequently on people's thermal sensation. In all urban areas, for NE–SW orientation the solar radiation has the highest impact on thermal discomfort at pedestrian level. Only in open-set high-rise urban areas the presence of the trees could locally reduce the human thermal stress at pedestrian level. This aspect should be taken into consideration for example during the urban design phase for new urban areas.

This latter consideration is one of the urban recommendations carried out from the analyses. Therefore, the municipality of the city could quantitatively and qualitatively consider which urban interventions should be prioritized in new and consolidated urban areas in order to guarantee thermal comfort at the pedestrian level. Future development of the study could include an economic evaluation to estimate the financial impact of each specific intervention.

6 Conclusion

In this deliverable, a number of urban planning strategies on a regional and district scale have been simulated.

A general conclusion regarding the methods and the tools for UHI characterization at different urban scales is that the multi-scale model approach could definitely offer a plausible and sophisticated pathway for UHI and urban climate change studies. A multi-scale approach combining mesoscale and microscale models represents a valuable methodology for having different types of analyses for different urban scales. It could be used for specific urban planning phases from zoning areas to urban canyon design and to provide urban design recommendations at different levels.

One of the limits of this approach is the high computational cost. However, as numerical modelling capabilities continue to improve for different scales and also become more accurate, lower computational costs and easier multi-model coupling will allow for significant improvements to nested modelling. From a practical perspective, for example, the boundary conditions could be forced on the microclimate model using the results from the mesoscale model. Therefore, multi-scale numerical studies that employ dynamic downscaling represent a promising tool for climatologists, meteorologists, urban planners, engineers and policymakers to evaluate climate change adaptation strategies in urban areas as well as for the future simulation of pedestrian comfort [60,113].

Although the representativeness of the case study cities is limited and has to be seen in the light of the modelling and specific meteorology boundary conditions, the findings suggest that applying vegetative measures inside urban street canyons can lead to noticeable reductions in air temperatures due to their cooling effect. The use of tree-lined streets is most promising.

The findings demonstrate that urban green areas such as parks and green infrastructure like tree-lined streets have the potential to reduce the UHI risk locally and in the nearby

areas. At the scale of an entire city, the effect of vegetation on air temperature appears to be limited, unless the percentage of urban vegetation is radically (and unrealistically) enhanced. Furthermore, when considering big parks (e.g. Antwerp), the effect on air temperature is limited to the very nearby areas. Urban materials and land use (building height and street aspect ratio) together with vegetation can influence urban surface temperatures, and consequently air temperatures as well as the characteristics of UHI.

Nevertheless, vegetation on the very local scale does have a good potential as a cooling measure, especially due to its influence on the radiation fluxes and consequently its impact on thermal comfort.

As a result, applying vegetative measures inside urban street canyons can be a relevant climate change adaptation strategy when designing liveable public spaces and/or walkable areas. The vegetation elements that look more promising are trees, preferably aligned, which provide local benefit, while grass can affect heat accumulation and help to maintain an adequate surface temperature both for the street and building walls. Additional benefits would be expected using green façades as they would reduce building energy consumption. This aspect is due to be studied in upcoming projects. Finally, the data has shown that the benefits of green roofs on thermal comfort at the very local scale are negligible.

Acknowledgments

The authors wish to thank the municipalities of Antwerp and Bilbao for supporting part of these studies through an active and constructive technical dialogue during the entire development of the work. For the Bilbao case study city, the authors also wish to thank the Environmental Department and the Basque Meteorological Agency in the Basque Country (Spain) for providing the climatic data.

References

[1] United Nations, Department of Economic and Social Affairs, Population Division, " World Urbanization Prospects: The 2011 Revision," 2012.

[2] L. Chen and E. Ng, "Outdoor thermal comfort and outdoor activities: A review of research in the past decade," *Cities,* vol. 29, pp. 118-125, 2012.

[3] P. Kastner-Klein, R. Berkowicz and R. Britter, "The influence of street architecture on flow and dispersion in street canyons," *Meteorology and Atmospheric Physics,* pp. 121-131, 2004.

[4] K. M. A. Gabriela and W. R. Endlicher, "Urban and rural mortality rates during heat waves in Berlin and Brandenburg, Germany," *Environmental Pollution,* pp. 2044-2050, 2011.

[5] B. Dousset, F. Gourmelon, K. Laaidi, A. Zeghnoun, E. Giraudet, P. Bretin, E. Mauri and S. Vandentorren, "Satellite monitoring of summer heat waves in the Paris metropolitan area," *Int J Climatol. 2011,* pp. 313-323, 2011.

[6] S. Vandentorren, F. Suzan, S. Medina, M. Pascal, A. Maulpoix, J. C. Cohen and M. Ledrans, "Mortality in 13 French cities during the August 2003 heatwave," *American Journal of Public Health,* vol. 94, pp. 1518-1520, 2004.

[7] R. C. Keller, Fatal isolation: The devastating Paris heat wave of 2003, Chicago: University of Chicago Press, 2015.

[8] G. A. Meehl and C. Tebaldi, "More intense, more frequent and longer lasting heat waves in the 21st century," *Nature,* vol. 305, pp. 994-997, 2004.

[9] N. S. Diffenbaugh and F. Giorgi, "Climate change hotspots in the CMIP5 global climate model ensemble," *Climatic Change,* vol. 114, pp. 813-822, 2012.

[10] C. Schär, P. L. Vidale, D. Lüthi, C. Frei, C. Häberli, M. A. Liniger and C. Appenzeller, "The role of increasing temperature variability in European summer heatwaves," *Nature 427,* pp. 332-336, 2004.

[11] K. A. Borden and S. L. Cutter, "Spatial patterns of natural hazards mortality in the United States," *International Journal of Health Geographics,* vol. 7, 2008.

[12] J. L. I. Beven, L. A. Avila, E. S. Blake, D. P. Brown, J. L. Franklin, R. D. Knabb, R. J. Pasch, J. R. Rhome and S. R. Stewart, "Atlantic Hurricane Season of 2005," *Mon. Wea. Rev.,* vol. 136, pp. 1109-1173, 2008.

[13] J. M. Robine, S. L. K. Cheung, S. Le Roy, H. Van Oyen, C. Griffiths, J. P. Michel and F. R. Herrmann, "Death toll exceeded 70,000 in Europe during the summer of 2003," *Comptes Rendus Biologies,* vol. 331, pp. 171-178, 2008.

[14] M. V. Saha, R. E. Davis and D. M. Hondula, "Mortality displacement as a function of heat event strength in 7 US cities," *American Journal of Epidemiology,* vol. 179, pp. 467-474, 2014.

[15] L. Toulemon and M. Barbieri, "The mortality impact of the August 2003 heat wave in France: Investigating the 'harvesting' effect and other long-term consequences," *Population Studies,* vol. 62, pp. 39-53, 2008.

[16] B. Stone, The city and the coming climate. Climate change in the places we live, Cambridge: Cambridge University Press, 2012.

[17] D. Li and E. Bou-Zeid, "Synergistic interactions between urban heat islands and heat waves: the impact in cities is larger than the sum of its parts," *Journal of Applied Meteorology and Climatology,* vol. 52, pp. 2051-2064, 2013.

[18] S. L. Harlan, A. J. Brazel, L. Prashad, W. L. Stefanov and L. Larsen, "Neighborhood microclimates and vulnerability to heat stress," *Social Science & Medicine, 63,* pp. 2847-2863, 2006.

[19] I. Zoulia, M. Santamouris and A. Dimoudi, "Monitoring the effect of urban green areas onthe heat island in Athens.," *Environmental Monitoring and Assessment, 156 (1-4),* pp. 275-292, 2009.

[20] J. Fallmann, S. Emeis and P. Suppan, "Mitigation of urban heat stress – a modelling case study for the area of Stuttgart," *DIE ERDE, 144, no. 3-4,* pp. 202-216, 2013.

[21] S. Schubert and S. Grossman-Clarke, "The Influence of Green Areas and Roof Albedos on Air Temperatures during Extreme Heat Events in Berlin," *Meteorologische Zeitschrift, 22 (2),* pp. 131-143, 2013.

[22] C. Yu and W. N. Hien, "Thermal benefits of city parks," *Energy and Buildings,* vol. 38, no. 2, pp. 105-120, 2006.

[23] T. R. Oke, "The micrometeorology of urban forest," *Philosophical Transactions of the Royal Society of London, Biological Sciences B,* pp. 335-349, 1989.

[24] L. Shashua-Bar and M. E. Hoffman, "Vegetation as a climatic component in the design of an urban street," *Energy and Buildings,* vol. 31, pp. 221-235, 2000.

[25] L. Shashua-Bar, O. Potchter, A. Bitan, D. Boltansky and Y. Yaakovet, "Microclimate modeling of street tree species effects within the varied urban morphology in the Mediterranean city of Tel Aviv, Israel," *International Journal of Climatology,* vol. 30, pp. 44-57, 2010.

[26] A. Dimoudi and M. Nikolopoulou, "Vegetation in the urban environments: micro-climatic analysis and benefits," *Energy and Buildings,* pp. 69-76, 2003.

[27] A. Chudnovsky, E. B. Dor and H. Saaroni, "Diurnal thermal behavior of selected urban objects using remote sensing measurements.," *Energy and Buildings,* pp. 1063-1074, 2004.

[28] D. Gromke, B. Blocken, W. Janssen, B. Merema, T. van Hooff and H. Timmermans, "CFD analysis of transpirational cooling by vegetation: Case study for specific meteorological conditions during a heat wave in Arnhem, Netherlands," *Building and Environment, 83,* pp. 11-26, 2015.

[29] S. E. Gill, J. F. Handley, A. R. Ennos and S. Pauleit, "Adapting Cities for Climate Change: The Role of the Green Infrastructure," *Built Environment, 33,* pp. 115-133, 2007.

[30] K. Axarli and A. Chatzidimitriou, "Redesigning Urban Open Spaces Based on Bioclimatic Criteria : Two squares in Thessaloniki , Greece," in *PLEA 2012 - 28th Conference, Opportunities, Limits & Needs Towards an environmentally responsible architecture*, Lima, 2012.

[31] J. Gehl and L. Gemzøe, Public spaces, public life, Copenhagen, Copenhagen: Danish Architectural Press and the Royal Danish Academy of Fine Arts, School of Architecture Publishers, 2004.

[32] T. R. Oke, "Urban climates and global environmental change," *Applied Climatology,* pp. 273-287, 1997.

[33] R. H. Matsuoka and R. Kaplan, "People needs in the urban landscape – analysis of landscape and urban planning contributions," *Landscape and Urban Planning,* pp. 7-19, 2008.

[34] Y. J. Huang, H. Akbari, H. Taha and A. H. Rosenfeld, "The potential of vegetation in reducing summer cooling loads in residential buildings," *Journal of Climate and Applied Meteorology,* pp. 1103-1116, 1987.

[35] H. Akbari, "Shade trees reduce building energy use and CO 2 emissions from power plants,"

Environmental pollution, vol. 116, pp. 119-126, 2002.

[36] M. Fahmy and S. Sharples, "On the development of an urban passive thermal comfort system in Cairo, Egypt," *Building and Environment,* pp. 1907-1916, 2009.

[37] I. Eliasson, I. Knez, U. Westerberg, S. Thorsson and F. Lindberg, "Climate and behaviour in a Nordic city," *Landscape and Urban Planning,* vol. 82, pp. 72-84, 2007.

[38] J. Zacharias, T. Stathopoulos and H. Wu, "Microclimate and downtown open space activity," *Environment and Behavior,* vol. 33, pp. 296-315, 2001.

[39] D. Alkam and M. Boukhabl, "Impact of Vegetation on Thermal Conditions Outside, Thermal Modeling of Urban Microclimate, Case Study: The Street of the Republic, Biskra," *Energy Procedia,* vol. 18, pp. 73-84, 2012.

[40] Y. Shapiro and Y. Epstein, "Environmental physiology and indoor climate - Thermoregulation and thermal comfort," *Energy and Buildings,* vol. 7, pp. 29-34, 1984.

[41] H. Hensel, "Thermal comfort in man," in *Thermo- reception and Temperature Regulation,* New York, Academic Press, 1981, pp. 168 - 184.

[42] S. Carr, M. Francis, L. G. Rivlin and A. M. Stone, Public space, Cambridge: Cambridge University Press, 1993.

[43] C. C. Marcus and C. Francis, People places – Design guidelines for urban open space, New York: Wiley & Sons, Inc., 1998.

[44] T. Maruani and I. Amit-Cohen, "Open space planning models: A review of approaches and methods," *Landscape and Urban Planning,* vol. 81, no. 1-2, pp. 1-13, 2007.

[45] T. P. Lin, A. Matzarakis and R. L. Hwang, "Shading effect on long-term outdoor thermal comfort," *Building and Environment,* vol. 45, no. 1, pp. 213-221, 2010.

[46] B. G. Gregoire and J. C. Clausen, "Effect of a modular extensive green roof on stormwater runoff and water quality," *Ecological Engineering, 37,* pp. 963-969, 2011.

[47] M. Aarts, M. Marijnissen, L. Stenhuijs, J. Borsboom, E. Rietveld, D. Doepel, J. Visschers and S. Lap, Rotterdam - People make the inner city, Rotterdam: Mediacenter Rotterdam, 2012.

[48] K. Steemers, "Energy and the city: density, buildings and transport," *Energy and Buildings,* vol. 35, pp. 3-14, 2003.

[49] A. Yezioro, I. G. Capeluto and E. Shaviv, "Design guidelines for appropriate insolation of urban squares," *Renewable Energy,* vol. 31, pp. 1011-1023, 2006.

[50] M. Bruse, "Simulating microscale climate interactions in complex terrain with a high-resolution numerical model: A case study for the Sydney CBD Area," in *International Conference on Urban Climatology & International Congress of Biometeorology,* Sydney, 1999.

[51] R. Emmanuel, H. Rosenlundb and E. Johansson, "Urban shading – a design option for the tropics? A study in Colombo, Sri Lanka," *International journal of climatology,* vol. 27, no. 14, pp. 1995-2004, 2007.

[52] M. Bruse and H. Fleer, "Simulating surface – plant–air interactions inside urban environments with a three dimensional numerical model," *Environmental Modelling & Software,* vol. 13, no. 3-4, pp. 373-384, 1998.

[53] J. Teller and S. Azar, "Townscope II-A computer system to support solar access decision-making," *Solar Energy,* vol. 70, no. 3, pp. 187-200, 2001.

[54] A. Matzarakis, "Application of the RayMan model in urban environments," in *Ninth Symposium on the Urban Environment,* Keystone (Colorado - USA), 2010.

[55] S. Thorsson, F. Lindberg, J. Björklund, B. Holmer and D. Rayner, "Potential changes in outdoor thermal comfort conditions in Gothenburg, Sweden due to climate change: the

influence of urban geometry," *International Journal of Climatology,* vol. 31, no. 2, pp. 324-335, 2011.

[56] C. Huizenga, Z. Hui and E. Arens, "A model of human physiology and comfort for assessing complex thermal environments," *Building and Environment,* vol. 36, no. 6, pp. 691-699, 2001.

[57] M. Bruse, "ITCM – A simple dynamic 2-node model of the human thermoregulatory system and its application in a multi-agent system," *Annual Meteorology,* vol. 41, pp. 398-401, 2005.

[58] S. Huttner, M. Bruse and P. Dostal, "Using ENVI-met to simulate the impact of global warming on the microclimate in central European cities," in *5th Japanese-German Meeting on Urban Climatology*, Freiburg, 2008.

[59] J. Arnfield, "Two Decades Of Urban Climate Research: A Review Of Turbulence, Exchanges Of Energy And Water, And The Urban Heat Island," *International Journal of Climatology,* vol. 23, pp. 1-26, 2003.

[60] A. Rasheed and D. Robinson, "Multiscale modelling of urban climate," in *Proceeding of Eleventh International IBPSA Conference*, Glasgow, Scotland, 2009.

[61] J. A. Acero, J. Arrizabalaga, S. Kupski and L. Katzschner, "Deriving an Urban Climate Map in coastal areas with complex terrain in the Basque Country (Spain)" *Urban Climate,* pp. 35-60, 2013.

[62] NASA, "ASTER - Advance Spaceborne Thermal Emission and Reflection Radiometer," 2012. [Online]. Available: https://asterweb.jpl.nasa.gov/. [Accessed 11 November 2015].

[63] NASA, "MODIS - Moderate Resolution Imaging Spectroradiometer," [Online]. Available: http://modis.gsfc.nasa.gov/tools/. [Accessed 11 November 2015].

[64] The Weather Research & Forecasting Model, "The Weather Research & Forecasting Model," [Online]. Available: http://www.wrf-model.org/index.php. [Accessed 11 November 2015].

[65] J. Baumüller, U. Hoffmann and U. Reuter, "Climate booklet for urban development, Ministry of Economy Baden-Wuerttemberg, Environmental Protection Department," [Online]. Available: http://www.staedtebauliche-klimafibel.de/Climate_Booklet/index-1.htm. [Accessed 7 December 2015].

[66] D. Scherer, U. Fehrenbach, H. D. Beha and E. Parlow, "Urban planning process," *Atmos. Environ.,* vol. 33, pp. 4185-4193, 1999.

[67] VDI-Guideline 3787, Part 1, Environmental Meteorology-Climate and Air Pollution Maps for Cities and Regions, Berlin: VDI, Beuth Verlag, 1997.

[68] E. Parlow, D. Scherer and U. Fehrenbach, "Climatic analyse map for grenchen und umgebung, CAMPAS, Klimaanalyse- und Planungshinweiskarten für den Kanton Solothurn," University of Basel, Basel, 2001.

[69] E. Parlow, D. Scherer, U. Fehrenbach, M. Föhner and H. D. Beha, "Analysis of the Regional Climate of Basel, Switzerland. Klimaanalyse der Region Basel – KABA," 1995. [Online]. Available: http://pages.unibas.ch/geo/mcr/Projects/KABA/index.en.htm. [Accessed 7 December 2015].

[70] C. Ren, E. Ng and L. Katzschner, "Urban climatic map studies: a review," *Int. J. Climatol,* vol. 31, pp. 2213-2233, 2010.

[71] L. Chen and E. Ng, "Quantitative urban climate mapping based on a geographical database: a simulation approach using Hong-Kong as a case study," *Int. J. Appl. Earth Obs.,* vol. 13, pp. 586-594, 2011.

[72] U. Korsholm, A. Baklanov, A. Gross and J. H. Sørensen, "On the importance of the meteorological coupling interval in air pollution modeling," *Atmos. Environ.,* 2008.

[73] A. Baklanov, P. Mestayer, A. Clappier, S. Zilitinkevich, S. Joffre, A. Mahura and N. W. Nielsen, "Towards improving the simulation of meteorological fields in urban areas through

updated advanced surface fluxes description," *Atmos. Chem. Phys.,* vol. 8, pp. 523-543, 2008.

[74] A. Baklanov, A. Gross and J. H. Sørensen, "Modelling and forecasting of regional and urban air quality and microclimate," *J. Computational Technologies,* vol. 9, pp. 82-97, 2004.

[75] A. Baklanov and U. Korsholm, "On-line integrated meteorological and chemical transport modelling: advantages and prospective," in *29th NATO/SPS International Technical Meeting on Air Pollution, Modelling and its Application*, University of Aveiro, Portugal, 2007.

[76] A. Martilli, A. Clappier and M. W. Rotach, "An Urban Surface Exchange Parameterisation for Mesoscale Models,," *Bound.-Lay Meteorol.,* vol. 104, pp. 261-304, 2002.

[77] L. Allen, F. Lingberg and C. S. B. Grimmond, "Global to city scale urban anthropogenic heat flux: model and variability," *Int. J. Climatol.,* vol. 31, pp. 1990-2005, 2011.

[78] K. De Ridder, D. Lauwaet and B. Maiheu, "UrbClim - A fast urban boundary layer climate model," *Urban Climate,* vol. 12, pp. 21-48, 2015.

[79] W. Schmidt, "Kleinklimatische Aufnahmen durch Temperaturfahren," *Temperaturfahren. Meteorologische Zeitschrift 47,* vol. 47, pp. 92-106, 1930.

[80] T. R. Oke and G. B. Maxwell, "Urban heat island dynamics in Montreal and Vancouver," *Atmos. Environ., 9,* pp. 191-200, 1975.

[81] M. Söderström and B. Magnusson, "Assessment of local agroclimatological conditions – a methodology," *Agricult. Forest Meteorol., 72,* pp. 243-260, 1995.

[82] G. Torbjörn, "Thermal mapping – a technique for road climatological studies," *Meteorol. Appl.,* vol. 6, pp. 385-394, 1999.

[83] P. M. Teillet, R. P. Gauthier and A. Chichagov, "Towards integrated earth sensing: the role of in situ sensing," in *First International Workshop on Future Intelligent Earth Observing Satellites (FIEOS).*

[84] P. O. Fanger, Thermal Comfort Analysis and Applications in Environmental Engineering, London: McGraw Hill, 1970.

[85] J. Guerra, R. Velazquez and D. Velazquez, "Thermal Comfort in Open Spaces," POLIS research internal report US/7/96, University of Sevilla, 1996.

[86] A. Matzarakis, F. Rutz and H. Mayer, "Modelling radiation fluxes in simple and complex environments - application of the RayMan model," *Int J Biometeorol,* vol. 51, pp. 323-334, 2007.

[87] "VDI 3789, Part 2: Environmental Meteorology, Interactions between Atmosphere and Surfaces; Calculation of the short and long-wave radiation.," VDI/DIN-Handbuch Reinhaltung der Luft, Band 1b, Düsseldorf, 1994.

[88] "VDI 1998. VDI 3787, Part I: Environmental meteorology, Methods for the human biometeorological evaluation of climate and air quality for the urban and regional planning at regional level. Part I: Climate," VDI/DIN-Handbuch Reinhaltung der Luft, Band 1b, Düsseldorf, 1998.

[89] A. Matzarakis, Die thermische Komponen-te des Stadtklimas, vol. 6, Freiburg: Ber. Meteorol. Inst. Univ., 2001.

[90] A. Matzarakis, F. Rutz and H. Mayer, "Modelling radiation fluxes in simple and complex environments - Basics of the RayMan model.," *International Journal of Biometeorology,* vol. 54, pp. 131-139, 2010.

[91] P. Höppe, "The physiological equivalent temperature – a universal index for the biometeorological assessment of the thermal environment," *Int J Biometeorol,* pp. 71-75, 1999.

[92] A. Matzarakis, H. Mayer and M. G. Iziomon, "Applications of a universal thermal index: physiological equivalent temperature," *Int. J. Biometeorol,* vol. 43, pp. 76-84, 1999.

[93] K. Nagano and T. Horikoshi, "New index indicating the universal and separate effects on human comfort under outdoor and non-uniform thermal conditions," *Energy and Buildings,* vol. 43, no. 7, pp. 1694-1701, 2011.

[94] A. Matzarakis, H. Mayer and M. Iziomon, "Heat stress in Greece. Applications of a universal thermal index: physiological equivalent temperature," *Int J Biometeorol,* vol. 43, pp. 76-84, 1999.

[95] G. Jendritzky, H. Menz, H. Schirmer and W. Schmidt-Kessen, Methodik zur raumbezogenen Bewertung der thermischen Komponente im Bioklima des Menschen, (Fortgeschriebenes Klima Michel-Modell). Beitr Akad Raumforsch Landesplan 114, 1990.

[96] A. Matzarakis and H. Mayer, "Heat stress in Greece," *International Journal of Biometeorology,* vol. 41, no. 1, pp. 34-39, 1997.

[97] C. E. A. Winslow, L. P. Herrington and A. P. Gagge, "A new method of partitional calorimetry," *Amer J Physiology ,* vol. 116, pp. 641-655, 1936.

[98] R. P. Clark and O. G. Edholm, Man and his thermal environment, London: E. Arnold, 1985.

[99] N. Schwarz, S. Lautenbach and R. Seppelt, "Exploring indicators for quantifying surface urban heat islands of European cities with MODIS land surface temperatures," *Remote sensing of Environment 115,* pp. 3175-3186, 2011.

[100] C. Zhao and al., "Urban planning indicators, morphology and climate indicators: A case study for a north-south transect of Beijing, China," *Building and Environment,* vol. 46, no. 5, pp. 1174-1183, 2011.

[101] Z. Guo and al, "Assess the effect of different degrees of urbanization on land surface temperature using remote sensing images," *Procedia Environmental Sciences,* vol. 13, pp. 935-942, 2012.

[102] J. Jiang and G. Tian, "Analysis of the impact of Land use/Land cover change on Land Surface Temperature with Remote Sensing," *Procedia Environmental Sciences,* vol. 2, pp. 571-575, 2010.

[103] R. Oltra-Carrió, J. A. Sobrino, B. Franch and F. Nerry, "Land surface emissivity retrieval from airborne sensor over urban areas," *Remote Sensing of Environment,* vol. 123, pp. 298-305, 2012.

[104] A. R. Gillespie, S. Rokugawa, S. J. Hook, T. Matsunaga and A. B. Kahle, "Temperature/Emissivity Separation Algorithm Theoretical Basis Document, Version 2.4," NASA, 1999.

[105] B. Maiheu, K. D. Ridder, B. Dousset, P. Manuta, G. Ceriola, M. Viel, I. A. Daglis and al., "Modelling air temperature via assimilation of satellite derived surface temperature within the Urban Heat Island Project," in *Proceedings of the Joint SIG workshop,* Gehnt, 2010.

[106] A. Doucet, N. De Freitas and N. J. Gordon, Sequential Monte Carlo Methods in Practice, New York: Springer-Verlag, 2001.

[107] I. Keramitsoglou, I. A. Daglis, V. Amiridis, N. Chrysoulakis, G. Ceriola, P. Manunta, B. Maiheu, K. De Ridder, D. Lauwaet and M. Paganini, "Evaluation of satellite-derived products for the characterization of the urban thermal environment," *Journal of Applied Remote Sensing,* vol. 6, 2012.

[108] I. Keramitsoglou, C. T. Kiranoudis, B. Maiheu, K. De Ridder, I. A. Daglis, P. Manunta and M. Paganini, "Heat wave hazard classification and risk assessment using artificial intelligence fuzzy logic," *Environmental Monitoring and Assessment,* 2013.

[109] T. Brandsma and J. P. Van der Meulen, "Thermometer screen intercomparison in De Bilt (the

Netherlands) – Part II: Description and modeling of mean temperature differences and extremes," *International Journey of Climatology,* vol. 28, pp. 389-400, 2008.

[110] G. Lobaccaro and J. A. Acero, "Comparative analysis of green actions to improve outdoor thermal comfort inside typical urban street canyons," *Urban Climate,* vol. 14, no. 2, pp. 251-267, 2015.

[111] J. A. Acero and K. Herranz-Pascual, "A comparison of thermal comfort conditions in four urban spaces by means of measurements and modelling technique," *Building and Environment,* Vols. 93, Part 2, pp. 245-257, 2015.

[112] Euskalmet, Basque Meteorological Agency, "Climatology year per year," Euskalmet, Basque Meteorological Agency, 2011. [Online]. Available: http://www.euskalmet.euskadi.eus/s07-5853x/es/contenidos/informacion/cli_2013/es_clieus/es_2013.html. [Accessed 25 February 2015].

[113] P. Conry, A. Sharma, M. Potosnak, J. Hellmann and H. J. S. Fernando, "Multi-scale study of Chicago heat island and the impacts of climate change," in *94th Annual Meeting of American Meteorological Society*, Atlanta, 2014.